Climate Dynamics (2006) 27: 401–420
DOI 10.1007/s00382-006-0140-x

D. B. Stephenson · V. Pavan · M. Collins
M. M. Junge · R. Quadrelli
Participating CMIP2 Modelling Groups

North Atlantic Oscillation response to transient greenhouse gas forcing and the impact on European winter climate: a CMIP2 multi-model assessment

Received: 4 November 2004 / Accepted: 1 March 2006 / Published online: 22 April 2006

Abstract This study investigates the response of wintertime North Atlantic Oscillation (NAO) to increasing concentrations of atmospheric carbon dioxide (CO_2) as simulated by 18 global coupled general circulation models that participated in phase 2 of the Coupled Model Intercomparison Project (CMIP2). NAO has been assessed in control and transient 80-year simulations produced by each model under constant forcing, and 1% per year increasing concentrations of CO_2, respectively. Although generally able to simulate the main features of NAO, the majority of models overestimate the observed mean wintertime NAO index of 8 hPa by 5–10 hPa. Furthermore, none of the models, in either the control or perturbed simulations, are able to reproduce decadal trends as strong as that seen in the observed NAO index from 1970–1995. Of the 15 models able to simulate the NAO pressure dipole, 13 predict a positive increase in NAO with increasing CO_2 concentrations. The magnitude of the response is generally small and highly model-dependent, which leads to large uncertainty in multi-model estimates such as the median estimate of 0.0061 ± 0.0036 hPa per $\%CO_2$. Although an increase of 0.61 hPa in NAO for a doubling in CO_2 represents only a relatively small shift of 0.18 standard deviations in the probability distribution of winter mean NAO, this can cause large relative increases in the probabilities of extreme values of NAO associated with damaging impacts. Despite the large differences in NAO responses, the models robustly predict similar statistically significant changes in winter mean temperature (warmer over most of Europe) and precipitation (an increase over Northern Europe). Although these changes present a pattern similar to that expected due to an increase in the NAO index, linear regression is used to show that the response is much greater than can be attributed to small increases in NAO. NAO trends are not the key contributor to model-predicted climate change in wintertime mean temperature and precipitation over Europe and the Mediterranean region. However, the models' inability to capture the observed decadal variability in NAO might also signify a major deficiency in their ability to simulate the NAO-related responses to climate change.

D. B. Stephenson (✉)
Department of Meteorology,
University of Reading, Reading, UK
E-mail: d.b.stephenson@reading.ac.uk

V. Pavan
ARPA-SIM, Viale Silvani 6, 40122 Bologna, Italy

M. Collins
Hadley Centre, Met Office, Exeter, UK

M. M. Junge
Meteorologisches Institut, Universität Hamburg,
Hamburg, Germany

R. Quadrelli
University of Washington, Seattle, WA, USA

1 Introduction

The North Atlantic Oscillation (NAO) has long been recognised as one of the most important global modes of climate variability (Wanner et al. 2001; Ambaum et al. 2001; Stephenson et al. 2002). It is the statistically and physically robust component of the leading pattern of Northern Hemisphere SLP variability known as the Northern Annular Mode (NAM)—previously referred to as the Arctic Oscillation (Thompson and Wallace 2001; Ambaum et al. 2001, 2002). In particular, NAO accounts for much inter-annual and decadal variance over the Euro-Atlantic region in seasonal means of many meteorological variables such as Sea Level Pressure (SLP), 2-metre surface air temperature and precipitation (Barnston and Livezey 1987; Lamb and Peppler 1987; Bojariu 1992; Deser and Blackmon 1993;

Hurrell 1995; Hurrell and van Loon 1997; Dai et al. 1997; Wibig 1999; Stephenson et al. 2000; Marshall et al. 2001; Branstator 2002). In addition to its impacts on seasonal means, NAO has also been shown to be an important factor for determining the frequency and intensity of extreme weather events. For example, 'cold events', freezing rain and blocking over Russia and France (Plaut and Simonnet 2001; Thompson and Wallace 2001), prolonged dry spells over the Iberian peninsula (Rodò et al. 1997), heavy rainfall events over Scotland (Conway et al. 1996; Alexander and Jones 2001) and the Mediterreanean region (Trigo et al. 2000), and sea wave heights in the Scandinavian and North Atlantic region (The WASA group 1998).

Several studies have investigated the ability of general circulation models to simulate NAO/NAM. Atmosphere-only general circulation models are able to reproduce the main spatial and temporal characteristics of NAO (Glowienka-Hense 1990; Cohen et al. 2005). Several studies of individual coupled models have confirmed that such models are also able to capture many aspects of the NAO/NAM patterns including the correlations with other fields such as temperature and precipitation (Pittalwala and Hameed 1991; Osborn et al. 1999; Ulbrich and Christoph 1999; Fyfe et al. 1999; Zhou et al. 2000; Furevik et al. 2003; Holland 2003; Liu et al. 2004; Hu and Wu 2004; Terray et al. 2004; Min et al. 2005). The NAO simulated by the ECHAM4 coupled model was not found to be sensitive to the choice of ocean model (Ulbrich and Christoph 1999). Although most coupled models appear to be able simulate the main features of NAO/NAM, there is much model-dependent variation in how the models simulate the amplitudes, spatial patterns, and future trends.

More recent studies have presented comprehensive multi-model investigations (Stephenson and Pavan 2003; Osborn 2004; Rauthe et al. 2004; Kuzmina et al. 2005). Stephenson and Pavan (2003) assessed the NAO signature in winter mean surface air temperatures simulated by 17 global coupled ocean–atmosphere models participating in the first phase of the Coupled Model Intercomparison Project (CMIP). Encouragingly, 13 out of 17 of the models captured the NAO surface temperature quadrupole pattern with centres of action over Northwest Europe, the northwest Atlantic, the southeastern USA, and the Middle East. Several of the models significantly overestimated the correlation between NAO and ENSO as was also noted by Osborn (2004) in his SLP NAO survey of seven coupled models. In addition, Osborn (2004) found that neither the internally generated NAO variability nor the NAO response to increasing greenhouse gas forcing simulated by seven coupled models were compatible with the observed variations in the winter SLP NAO, particularly the positive trend from the 1960s to the 1990s (Feldstein 2002). The NAO response was found to be model-dependent and sensitive to the index used to measure it. Rauthe et al. (2004) investigated global warming trends in NAM in an inter-comparison study of nine coupled models perturbed with different greenhouse gas and sulphate aerosol forcings. Most climate models were found to predict positive NAM trends into the twenty-first century, whereas the NAO showed only weak positive and negative trends in different models and was less sensitive to radiative forcing. Kuzmina et al. (2005) surveyed 12 coupled models and found that the observed temporal trend in the NAO in recent decades lies beyond the natural variability found in the model control runs. For the majority of the models, a significant increase was found in the NAO trend in the forced runs relative to the control runs, suggesting that the NAO may intensify with further increases in greenhouse-gas concentrations.

In summary, although models appear to be able to simulate the main features of inter-annual variability in winter NAO, they underestimate the decadal trends that have been observed to occur in NAO (e.g. Osborn et al. 1999; Zorita and Gonzàlez-Rouco 2000; Gillett et al. 2002; Osborn 2002). Such trends could be of stochastic origin due to natural variability of the climate system (Stephenson et al. 2000; Slonosky and Yiou 2001; Paeth et al. 1999; Mosedale et al. 2005) and/or due to deterministic forcing factors such as greenhouse gas increases, depletion of the ozone hole, increases in aerosols etc. The return to less positive NAO winters after 1995 now casts some doubt on whether the 1960–1990s positive trend is related to anthropogenic climate change. This suggests that either climate models are not correctly representing the processes that lead to natural NAO variability, or alternatively are missing key important NAO forcing factors. Recent modeling studies have started to investigate the dependence of NAO/NAM on forcing factors such as low-latitude sea surface temperatures (Hurrell et al. 2004; Mosedale et al. 2005), sea-ice (Kvamsto et al. 2004; Alexander et al. 2004), snow-cover (Cohen et al. 2005), the stratosphere (Castanheira and Graf 2003; Scaife et al. 2005), and volcanic aerosols (Stenchikov et al. 2002). Significantly, Scaife et al. (2005) demonstrated that observed NAO trends could be reproduced in a GCM forced by observed trends in the stratosphere.

The main aims of this study are to (a) quantify the effect of greenhouse gases on NAO as simulated by 18 different coupled models, and (b) investigate the impact of this effect on European temperature and precipitation changes. Previous NAO modelling studies have suggested that the mean pattern of NAO is likely to strengthen rather than weaken with greenhouse gas increases but have not carefully quantified the magnitude of the response. Due to large model differences in NAO response, it is difficult to quantify the size of the effect when using only a small number of models (e.g. less than 10). This study uses 18 models and robust statistical techniques to provide a best estimate for the sensitivity of NAO to changes in atmosphere carbon dioxide concentration. The study then asks what the impact of these changes will be on winter mean temperatures and precipitation in the Northern Hemisphere, and in particular in Europe. Using a regression model, Hurrell (1995)

argued that observed NAO trends could be used to explain recent warming and precipitation trends over Europe. However, more recent studies have suggested that regional warming trends in Norway and over the Arctic cannot be fully explained by NAO/NAM (Benestad 2001; Overland and Wang 2005). This important issue is addressed here using the large data set provided by this set of coupled model simulations.

This paper is structured as follows. Section 2 describes the definition of NAO index used in this study and the coupled model experiments. The behaviour of NAO in the different models is described in Sect. 3. Section 4 then presents the model predicted changes in winter mean temperature and precipitation and uses a linear regression model to assess how much of the changes can be accounted for by the changes seen in NAO. Section 5 concludes the paper with a summary of the main findings and a brief discussion of the implications for understanding future climate change.

2 Definition of NAO and coupled model experiments

2.1 A simple NAO index and its covariability with European climate

Figure 1 summarises the main features of the winter NAO evolution from 1900–2004 and its statistical relationship with European climate. The NAO index in Fig. 1a was computed from observational gridded mean sea level pressure data (Trenberth and Paolino 1980), and then covariances were calculated between this index and observed winter mean precipitation from 1979–1995 (Xie and Arkin 1996) and observed winter mean surface temperatures from 1900–1994 (Jones et al. 1986).

The NAO index is defined in this study as the difference between the December–February mean SLP spatially averaged over two large rectangular latitude–longitude regions: a subtropical Mid-Atlantic and Southern Europe region (90W–60E, 20N–55N) and a North Atlantic–Northern Europe region (90W–60E, 55N–90N). Unlike 2-point indices, this simple area average definition of NAO index uses SLP information covering a large part of the Atlantic from the tropics up to the North Pole (90W–60E, 20–90N) and is robust to modest changes in the position of centres of action in the observations and models. Furthermore, this definition avoids ambiguity and interpretation problems that occur when using more sophisticated definitions such as those based on principal component analysis (Osborn et al. 1999; Ambaum et al. 2001; Wanner et al. 2001). The analysis presented in this paper has been repeated using various NAO indices defined over smaller areas and similar conclusions were obtained (not shown).

As discussed in many studies (e.g. Hurrell 1995; Hurrell and van Loon 1997), winter mean NAO has strong associations with winter mean temperature and precipitation in Europe. The covariance maps in Fig. 1b and c reveal that positive NAO conditions are associated with increased precipitation over Northern Europe, decreased precipitation over Southern Europe and the Mediteranean region, and increased surface tempera-

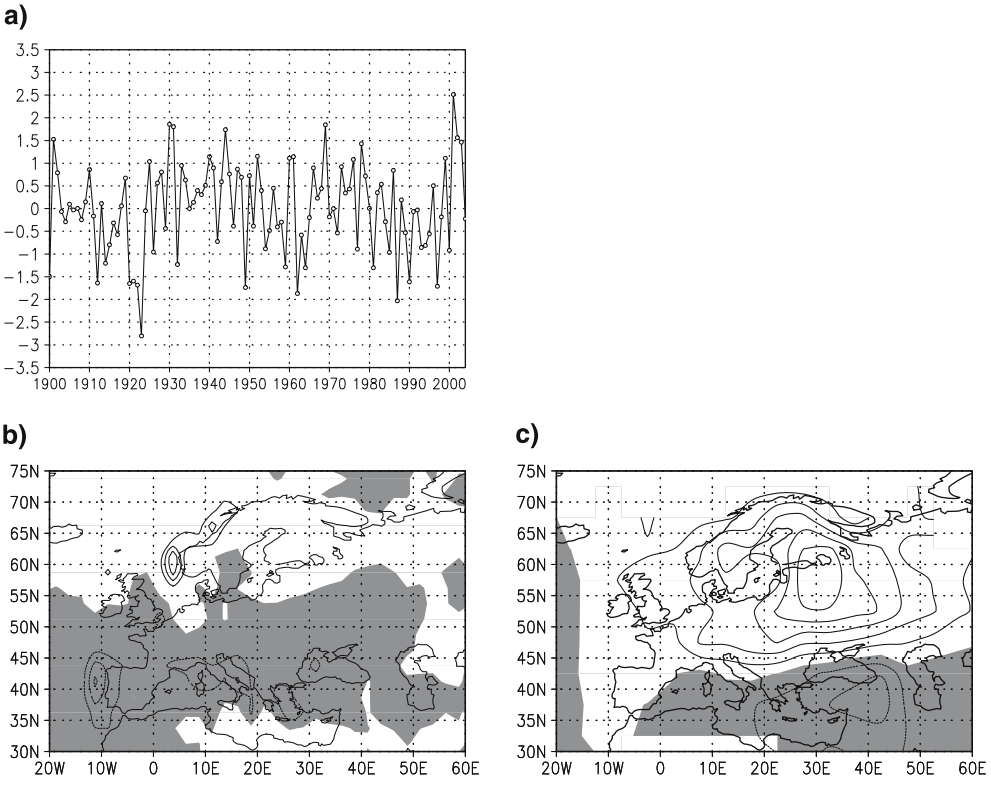

Fig. 1 **a** Time series of the standardised NAO index for winters from 1900/1 to 2004/5, **b** covariance of winter mean precipitation and NAO (contour interval 0.5 mm/day, negative area *shaded*, negative contours *dashed*), **c** covariance of winter mean surface temperature and NAO (contour interval 0.1°C, negative values *shaded*, negative contours *dashed*)

Table 1 Summary of the CMIP2 models used in this study

Model name	Atmospheric model horizontal truncation and resolution (in degrees)	Flux correction	Control run length (in years)	Perturbed run length (in years)
BMRC2	R21 ~5.6×3.2	Heat, water, sfc SW radn.	80	80
CCCma1	T32 ~3.8×3.8	Heat, water	80	80
CCSR	T21 ~5.6×5.6	Heat, water	80	80
CERFACS2	T32 ~3.8×3.8	–	80	80
CSIRO	R21 ~5.6×3.2	Heat, water, and momentum	80	80
ECHAM3	T21 ~5.6×5.6	Heat, water, and momentum	80	80
ECHAM4	T42 ~2.8×2.8	Heat, water (annual mean)	80	80
GFDL_R15a	R15 ~7.5×4.5	Heat, water	80	80
GISS	5.0×4.0	–	75	80
IAP/LASG2	R15 ~7.5×4.5	Heat, water, and momentum	80	80
INMCM	5.0×4.0	–	80	80
LMD/IPSL2	5.6×3.2	–	80	80
MRI2	5.0×4.0	Heat, water	80	80
NCAR_CSM	T42 ~2.8×2.8	–	80	80
NCAR_WM	R15 ~7.5×4.5	–	75	75
DOE_PCM	T42 ~2.8×2.8	–	80	80
HADCM2	3.75×2.5	Heat, water	80	80
HADCM3	3.75×2.5	–	80	80

tures over Northern and Central Europe. Hence, recent trends in NAO have been invoked to account for recent warming and precipitation trends in Europe suspected to be attributable to anthropogenic global warming (Hurrell 1995; Paeth et al. 1999). However, it should be noted that other large-scale factors such as the Cold Ocean Warm Land pattern have also been suggested as possible candidates for explaining decadal temperature trends (Wallace et al. 1996).

2.2 The coupled model experiments

Phase 2 of the Coupled Model Intercomparison Project (CMIP2) was designed to assess the response of fully coupled general circulation model simulations to transient increasing concentrations of atmospheric CO_2 (Meehl et al. 2000). Each participating institution produced two experiments using the same coupled global circulation model: a control and a perturbed experiment. The control experiment (CON) consists of a simulation of at least 80 years in length in which the atmospheric CO_2 concentration is constant and equal to its preindustrial or present-day value. The perturbed experiment (PER) is integrated for the same number of years as the control, using an identical experimental set-up, but with a 1% per year compounded increase in CO_2 concentrations. Doubling of atmospheric CO_2 concentration occurs at around year 70 of the PERs.

Monthly mean grid point fields of sea level pressure, surface air temperature, and precipitation were made available from coupled models run at the following institutions: Bureau of Meteorology Research Center (BMRC2, Australia), Canadian Centre for Climate Modelling and Analysis (CCCma1, Canada), Center for Climate System Research (CCSR, Japan), CERFACS (CERFACS2, France), CSIRO (CSIRO, Australia), ECHAM3 + LSG from DKRZ/MPI (ECHAM3, Germany), ECHAM4 + OPYC3 also from DKRZ/MPI (ECHAM4, Germany), Geophysical Fluid Dynamic Laboratory (GFDL_R15a, USA), NASA GISS Russell model (GISS, USA), LASG/ Institute for Atmospheric Physics (IAP/LASG2, China), Institute of Numerical Mathematics (INMCM, Russia), LMD (LMD/IPSL2, France), Meteorological Research Institute (MRI2, Japan), NCAR CSM (NCAR_CSM, USA), NCAR Washington and Meehl model (NCAR_WM, USA), the Naval Research Laboratory, Monterey (NRL, USA), DOE Parallel Climate Model (DOE_PCM, USA), HadCM2 model (HADCM2, UK), and HadCM3 model (HADCM3, UK). Although some records of GISS sea level pressure data were irreparably damaged during central archiving, the remaining data from these simulations were included in this study. The simulations from the NCAR_WM were also slightly shorter than 80 years, but have been included in our analysis. Finally, data from the NRL model contained only 3 years of 'control' integration and so were not included. Table 1 summarises the main characteristics of the models, including their horizontal resolution, the use of flux adjustment (if any) and the duration of the experiments.

Although the CMIP2 model simulations were produced several years ago, they are still representative of the global climate simulations now used to produce climate change projections. An important aspect of the CMIP2 design of experiments is that the different model simulations are directly comparable, since they were all forced with exactly the same atmospheric CO_2 concentrations and were run for the same number of years. As a consequence, it is possible to combine the results obtained from different models within this project and obtain answers which are, to some extent, model

independent. This multi-model combination approach has already been shown to give improved results when applied to other weather and climate prediction pro0000blems such as medium-range weather forecasts (Harrison et al. 1996) and seasonal forecasting (Pavan et al. 2005; Doblas-Reyes et al. 2003; Gillett et al. 2002; Palmer et al. 2000; Pavan and Doblas-Reyes 2000; Krishnamurti et al. 1999).

A limitation of the CMIP2 simulations is the idealised nature of the greenhouse gas perturbations. The perturbation includes only changes in CO_2 concentrations, and disregards all other possible anthropogenic forcing, such as changes in the concentration of other greenhouse gases (e.g. methane), aerosols, and ozone. As a consequence, the results of this study should not be taken as perfect forecasts of future climate since other factors will undoubtedly also be important. It remains an interesting area for future research as to how NAO will respond to these other forcing factors.

3 Model simulation of NAO

This section examines the variability and trends in NAO indices calculated for each of the 18 model simulations using the identical area-average approach to that used for the observations discussed in Sect. 2.1.

3.1 How well do the models capture the NAO spatial pattern?

The first question to be considered is how well the models reproduce the observed NAO variability under 'control' conditions. During the first phase CMIP1, Stephenson and Pavan (2003) found that all the available models captured the presence of the well-known NAO-related dipole in temperature between Greenland and northern Europe. Because sea level pressure was not made available in CMIP1, they used this temperature dipole to

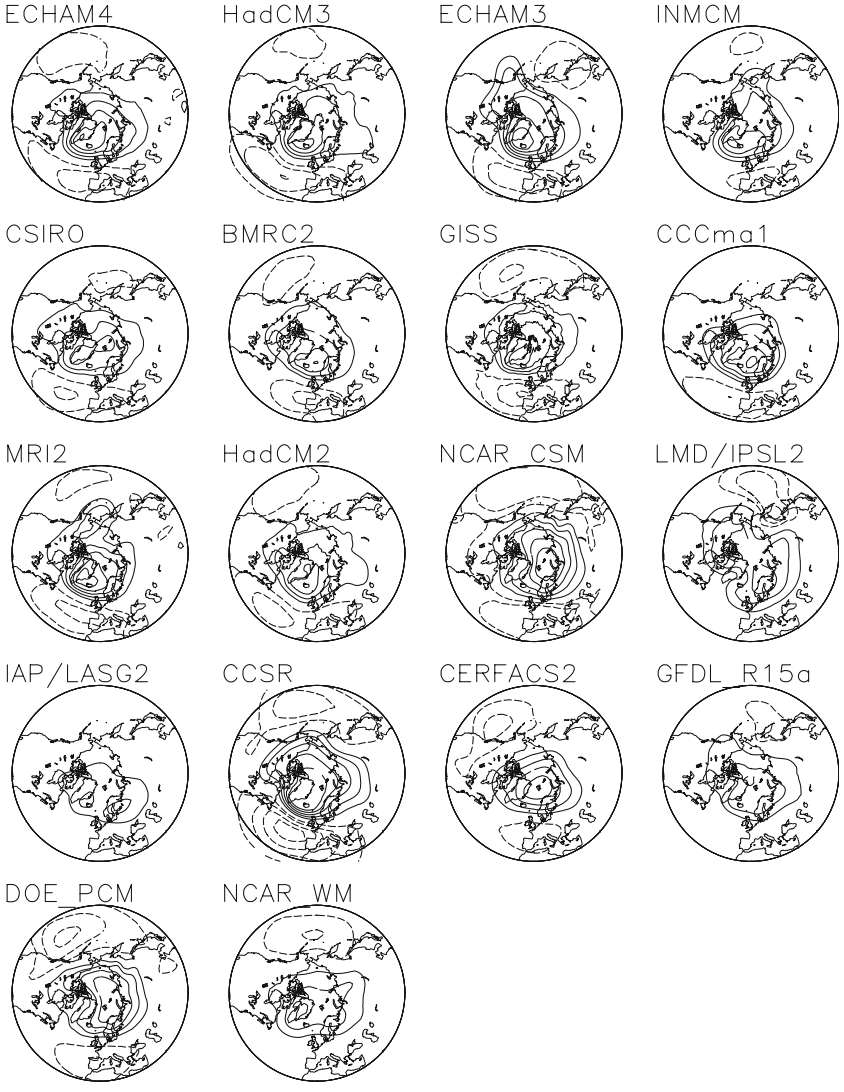

Fig. 2 Maps of covariance between SLP grid point values and the standardised northern box SLP indices for each of the control simulations. Contour interval of 1 hPa from −5 to 5 hPa with the zero contour line not shown. Positive contours are *solid*, negative are *dashed*

define an NAO index similar to that used in early twentieth century NAO studies (Stephenson et al. 2002).

Before defining an NAO index based on the difference between sub-tropical and high-latitude SLP, it is necessary to investigate how well models capture the north-south NAO dipole in SLP in the Atlantic sector. Figure 2 shows maps of covariance for each model between winter-mean SLP and an index obtained by averaging SLP over the northern box (90W–60E, 55N–90N). All but three models (GFDL_R15a, IAP/LASG2 and NCAR_WM) are able to qualitatively reproduce the observed north-south NAO dipole pattern. In three remaining models (LMD/IPSL2, GFDL_R15a and NCAR_WM) the region of negative covariance over the Pacific is the only one characterised by a sea-saw in SLP. Apart from the CCCma1 model, all other models characterised by a sea-saw of SLP over the North Atlantic, present also a region of negative covariance over the Pacific. In 13 models, the covariance map shows positive values extended to the whole Arctic region but with greater amplitude over the North Atlantic and Greenland similar to that seen in observed NAO. In three models (NCAR_CSM, CERFACS2 and DOE_PCM), the pattern presents a maximum located over the Arctic, north of Siberia, while in one model (IAP/LARG2) the pattern presents an extended but weak vortex with two maxima one between Greenland and Iceland, the other over Scandinavia.

3.2 Exploratory analysis of the model NAO indices

An NAO index has been calculated for each of the model simulations by taking the difference between the December-February mean SLP spatially averaged over the North Atlantic-Northern Europe region (90W–60E, 55N–90N), and the mid-Atlantic-Southern Europe region (90W–60E, 20N–55N). Figure 3 shows time series plots of centred NAO indices simulated by each of the models, and for comparison, the observed NAO index (computed from box averages of the observational gridded mean sea level pressure data set of Trenberth and Paolino 1980). This complex multi-model sample of $18\times(80+80)=2{,}880$ winter NAO values requires careful analysis in order to draw correct inferences about future probable values of NAO.

For the model simulations, the first 80 years are the values from the control simulation that had constant

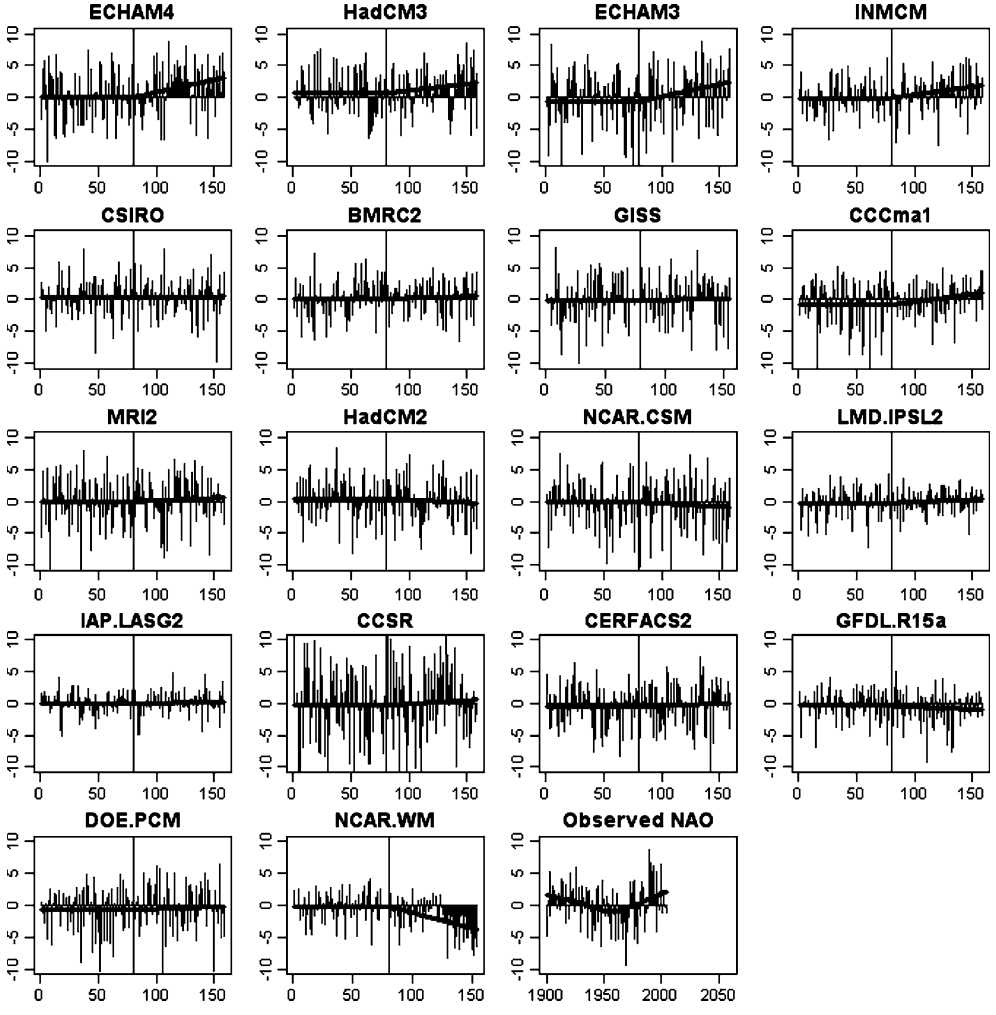

Fig. 3 Time series plots of the NAO indices simulated by the 18 models, and for comparison the time series of the observed index from 1920 to 2000 (in units of hPa). The first 80 years of the simulated indices are from the control runs having a constant carbon dioxide concentration and the following 80 years were made by increasing carbon dioxide concentration at 1% per year. Each index has been centred by removing the median value of NAO over the control run (the first 80 years). The *thick solid lines* show trends estimated using piecewise linear regression for the simulated indices and a local non-linear (lowess) regression for the observations (see text for details)

present-day carbon-dioxide concentration, and then the following 80 years are from the runs that had the carbon dioxide concentration increasing at 1% per year. The time series have been centred (bias corrected) by subtracting out the median over the first 80 years so that all the models have zero median during the control run. The models have been sorted in order of decreasing change in the median between the increasing carbon dioxide and control simulations.

The time series exhibit a large amount of irregular year to year variation superimposed on smaller longer term trends (thick solid lines—explained in the following section). In general, the models simulate the irregular variations with similar magnitude to those seen in the observations. Notable exceptions are the CCSR model that has too much NAO variability and IAP/LASG2 that has too little. The majority of models show either very small or slightly increasing trends in NAO during years 81–160, however, two models (NCAR_WM and GFDL_R15a) simulate decreasing trends. The rate of change of the trends varies widely between the models and none of the model trends has as large a rate of change as the increasing trend that occurred in the observed index from 1960 to the mid-1990s. However, it should also be noted that since the mid-1990s the increasing trend in the observed NAO index has declined. This is consistent with the suggestion that such trends in the observed NAO are stochastic natural variability having long-range dependence (Stephenson et al. 2000; Mosedale et al. 2006). From Fig. 3, it is clear that all the 18 models underestimate the low-frequency variability in NAO. This underestimation of decadal variability in the model simulated NAO series could help explain why the 1960–1990 increasing trend in NAO has being attributed to anthropogenic climate change (e.g. Gillett et al. 2003). However, it should be remembered that these simulations do not include natural variations in external forcing, which are present in the real climate such as volcanism and solar variations.

Figure 4 shows notched box-and-whisker plots that summarise the different simulations and observations.

Box-and-whisker plots (or box plots) are a simple robust way of summarising data based on resistant (i.e. not unduly affected by outlier values) quartile measures rather than on the non-resistant measures of mean and standard deviation (Chambers et al. 1983). The box denotes the central location of the data by a mid-line at the median value, and the scale (spread) of the data by hinge lines at the lower and upper quartiles—half the sample values lie within the box. The notches on the box give roughly a 95% confidence interval for the difference in two medians. They extend to $\pm 1.58 IQR/\sqrt{n}$ from the

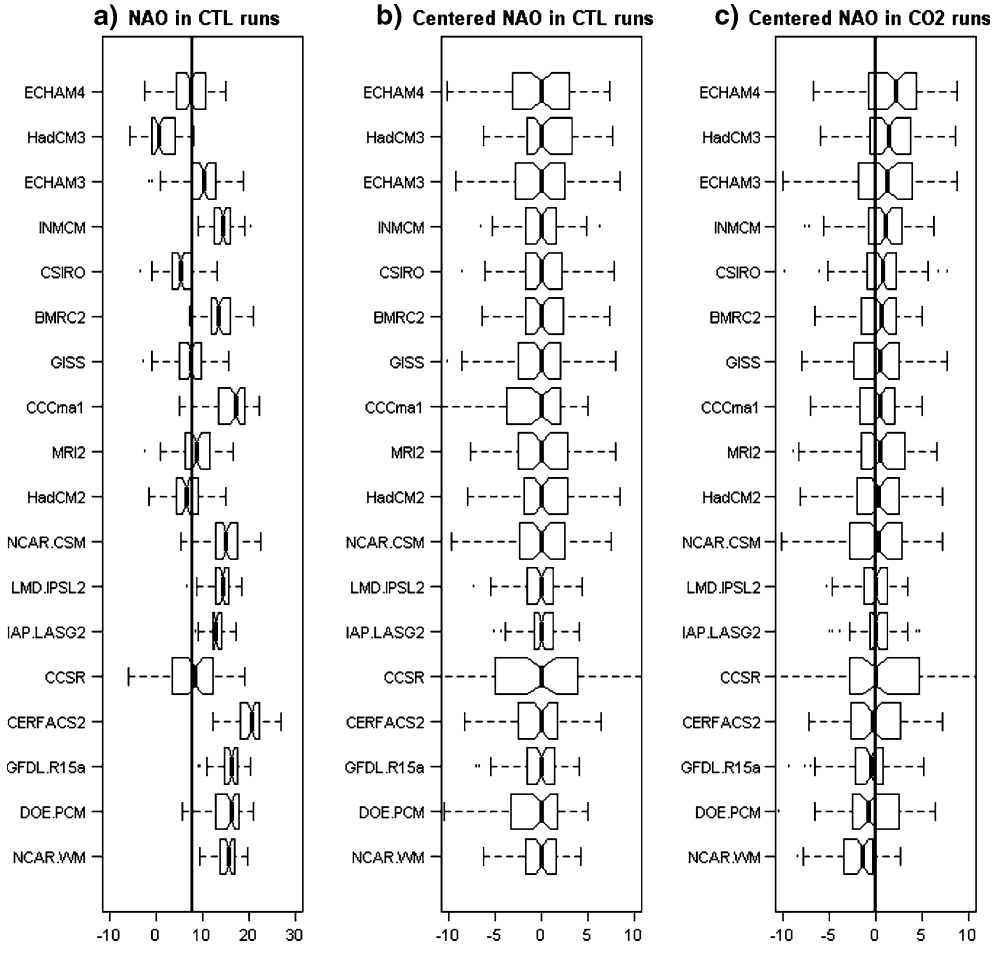

Fig. 4 Summary notched box-and-whisker plots for: **a** the NAO indices in the 80 years of control run (*the solid vertical line* marks the median of the observed NAO index from 1920–2000), **b** the NAO indices from the control run centred by removing the median value over each control run, **c** the NAO indices from the doubling carbon dioxide runs centred by removing the median value over each control run (*the solid vertical line* shows the median centred value of zero from the control runs)

median where IQR is the Inter-Quartile Range (the difference between the 75th and 25th percentiles) assuming asymptotic normality of the median and roughly equal sample sizes for the two medians being compared (Chambers et al. 1983, p. 62). The whiskers extend to the most extreme data values not more than 1.5 times the inter-quartile range from the respective hinges. Dots outside the whiskers denote potentially suspicious outlier values.

Figure 4a shows that the indices simulated in the control runs have a wide spread about the median of the observed NAO index. In general, most of the models have NAO indices that are larger than the median of the observed NAO index equal to 7.94 hPa. HadCM3 and CSIRO are notable exceptions in that their NAO indices are centred below the observed value. Several of the models have median values of NAO that are twice that observed indicating a model bias towards unrealistically strong westerly flow in the Atlantic region.

Figure 4b shows box plots for NAO indices from the control runs centred by subtracting out their respective medians. This crude form of bias correction considerably reduces the model spread noted in Fig. 4a. Many of the models have inter-quartile ranges similar to the inter-quartile range of 4.37 hPa obtained for the observed index NAO from 1920 to 2000. CCSR and IAP/LASG2 stand out as obvious outliers having too much and too little spread, respectively.

Figure 4c shows box plots for centred NAO indices from the increasing carbon dioxide simulations (years 81–160). The changes in median from the control run can be noted in the displacement of box plot mid-lines from the thick vertical zero line. Judging by the notches on the box plots, several models show a statistically significant (at the 5% level) increase in the median (ECHAM4, HadCM3, ECHAM3, INMCM, CSIRO, BMRC2) whereas several other models show a statistically significant decrease (GFDL_R15a, DOE_PCM, NCAR_WM). However, only one of the models with a decrease was able to simulate the NAO Atlantic pressure dipole. The width of the box plots shows little change from those in Fig. 3b indicating no substantial changes in NAO variability between the control and increasing carbon dioxide runs.

3.3 Estimation of NAO sensitivity to CO_2 changes

To quantitatively assess the sensitivity of NAO to changes in carbon dioxide concentration, it is necessary to fit appropriate trend models to the indices data. The simplest trend model assumes that NAO is the sum of a trend component in the mean and an irregular natural variability component. For the trend component, it is reasonable to assume that for small perturbations, the mean NAO is linearly related to the radiative greenhouse gas forcing, which is approximately proportional to the logarithm of the carbon dioxide concentration. Hence, the NAO index $Y(t)$ in year t can be modelled as the additive combination of a trend and noise component:

$$Y(t) = \beta_0 + \beta_1 \log \frac{CO_2(t)}{CO_2(t_0)} + \varepsilon(t) \quad (1)$$

where the regression slope parameter β_1 quantifies the sensitivity of NAO to carbon dioxide, and $\varepsilon(t)$ is a noise component that accounts for natural variability about the trend in the mean. For the NAO series shown in Fig. 3, the logarithm of carbon dioxide concentration is zero for years 1–80 and then increases linearly at a rate of log(1.01) per year for years 81–160. A 1% change in CO_2 concentration corresponds to almost a 1% change in $\log(CO_2)$ since $\log(1.01) = 0.00995$. Hence, to good approximation, the regression slope parameter β_1 can be considered to have units of hPa per $\%CO_2$. If one assumes that the noise component is Gaussian and serially uncorrelated, then this model can be fitted to the data using ordinary least-squares (OLS) piecewise linear (broken stick) regression of NAO on year.

However, such a trend model is overly restrictive in that it does not allow for the possibility of serial correlation in the irregular component, which is clearly evident as multi-year clustering (decadal variability) in several of the plots shown in Fig. 3 (e.g. the ECHAM3 simulation). It is therefore advisable to use generalised least-squares (GLS) regression that allows for correlation structure in the noise component (Draper and Smith 1998). In this study, we have assumed that the noise component can be modelled by an AR(1) process of the form $\varepsilon(t+1) = \rho\varepsilon(t) + \eta(t)$ where ρ is the lag-1 autocorrelation parameter for the noise component and $\eta(t)$ is Gaussian white noise. GLS is used in this study to simultaneously estimate the four model parameters β_0, β_1, σ_ε, ρ and their standard errors for each of the NAO indices. This was performed using the gls function in the nlme package of the free statistical language R—see http://www.r-project.org. The fraction of total variance R^2 explained by the trend and the statistical significance of the sensitivity β_1 being non-zero was also calculated.

The GLS estimated piecewise linear trends are shown on Fig. 3 as thick lines and the estimated parameters are given in Table 2. The trend shown on the time series plots of the observed NAO index has been estimated using a local non-linear robust smoothing fit known as LOWESS (Cleveland 1979). The NAO sensitivity estimates range from −0.00494 to 0.00396 hPa per $\%CO_2$ with typical standard errors on each model estimate of around 0.001 hPa per $\%CO_2$. Hence, the major source of uncertainty in estimating NAO sensitivity to greenhouse gas forcing is due to differences between the models rather than uncertainty arising from estimating trends over a finite 80 year long simulation period. The variation between model sensitivities is larger than can be explained by sampling uncertainties in the trend estimates. Only 4 out of 18 of the models have negative sensitivities (NCAR_WM, NCAR_CSM, HadCM2, and GFDL_R15a) yet it should be remembered that two of

these models (NCAR_WM and GFDL_R15a) were among the three models that were unable to reproduce the NAO SLP dipole. The lag-1 autocorrelation of the noise component is generally close to zero (white noise) except for ECHAM3 and IAP/LASG2 where it is small and positive and GFDL_R15a and DOE_PCM where it is small and negative. The small negative 1-year autocorrelation indicates the presence of an unexplained quasi-biennial component in these simulations. In all but one model (NCAR_WM), the trend component accounts for less than 10% of the total variance. The NAO sensitivity is significantly different from zero at the 5% level (p value ≤ 0.05) in only six of the models: ECHAM4, HadCM3, ECHAM3, INMCM, CCCma1 (positive trend) and NCAR_WM (negative trend).

Figure 5 shows a non-parametric kernel density estimate of the probability density function of model sensitivity estimates. The probability density function was estimated robustly by smoothing the data points using a local filter (the kernel) having an optimal bandwidth (Venables and Ripley 2002). The outlier model points were not found to have a major influence on the density estimate in the central part of the distribution where the bulk of the models are located. There is a wide spread in the distribution and it has fatter tails than a Normal distribution due to the outlier models. To infer the best point estimate of NAO sensitivity to greenhouse gas concentration, it is necessary to summarise this distribution.

A simple robust way to do this is to calculate empirical quantiles of the 18 sensitivity estimates. The median estimate of all the model sensitivities is 0.0061 hPa per $\%CO_2$. Therefore, there is probability of 0.5 that NAO will increase by more than 0.61 hPa for a doubling (100% increase) in carbon dioxide concentration. Although this represents only a relatively small shift of $0.61/3.36 = 0.18$ standard deviations in the probability distribution of NAO, it would lead to large relative increases in the probabilities of extreme values of NAO associated with damaging events such as severe European storms. The multi-model estimate is insensitive to the omission of outlier models, for example, the model median changes to 0.0059 hPa per $\%CO_2$ when ECHAM4 is omitted and 0.0062 hPa per $\%CO_2$ when NCAR_WM is omitted. The median estimate increases slightly to 0.0072 hPa per $\%$ CO_2 if the three models without NAO pressure dipole are removed (GFDL_R15a, IAP/LASG, and NCAR_WM).

An approximate 95% confidence interval for this estimate can be obtained by calculating the standard error in the median using $0.92IQR/\sqrt{m}$ based on the assumption that the $m = 18$ model sensitivities (in column 2 of Table 2) with Inter-Quartile Range (IQR; the difference between the 75th and 25th percentiles) of 0.0164 hPa per $\%CO_2$ are independent and normally distributed. This yields a lower bound estimate of the standard error in the model median of 0.0036 hPa per $\%CO_2$ that then gives a narrow estimate of the 95% confidence interval for NAO sensitivity of −0.0009–0.0131 hPa per $\%CO_2$. The true confidence interval is likely to be larger than this since the model sensitivities are neither independent nor normally distributed. Since even this interval includes zero, the null hypothesis that there is no effect of carbon dioxide on NAO cannot be

Table 2 Summary of piecewise linear trend fits to the simulated NAO indices

Model	Sensitivity $\hat{\beta}$	$s_{\hat{\beta}}$	S_ε	$\hat{\rho}$	p value	R^2 (%)
ECHAM4	**3.96**	**1.13**	**3.65**	**−0.01**	**< 0.01**	**7.80**
HadCM3	**2.09**	**1.05**	**3.18**	**0.06**	**0.05**	**3.37**
ECHAM3	**3.84**	**1.45**	**4.05**	**0.14**	**0.01**	**6.05**
INMCM	**2.47**	**0.84**	**2.69**	**0.01**	**< 0.01**	**5.85**
CSIRO	0.23	0.89	2.91	−0.02	0.79	0.68
BMRC2	0.50	0.83	2.71	−0.02	0.55	0.86
GISS	0.42	1.09	3.46	−0.07	0.70	0.77
CCCma1	**2.44**	**0.93**	**3.18**	**−0.07**	**0.01**	**4.38**
MRI2	0.79	1.06	3.68	−0.08	0.46	0.92
HadCM2	−0.82	1.03	3.26	0.01	0.43	1.04
NCAR_CSM	−0.96	1.18	3.96	−0.05	0.41	1.03
LMD/IPSL2	0.72	0.62	2.08	−0.05	0.24	1.43
IAP_LASG2	0.22	0.59	1.73	0.09	0.72	0.75
CCSR	1.18	1.96	5.80	0.08	0.55	0.91
CERFACS2	0.62	1.08	3.37	0.02	0.57	0.85
GFDL_R15a	−0.80	0.67	2.43	−0.13	0.23	1.37
DOE_PCM	0.59	0.92	3.37	−0.14	0.52	0.84
NCAR_WM	**−4.94**	**0.76**	**2.22**	**−0.01**	**< 0.01**	**22.80**

Bold shading indicates that the model has a non-zero sensitivity that is statistically significant at the 5% level. The parameters are given in the following units: NAO sensitivity to carbon dioxide concentration $\hat{\beta}_1$ in hPa/100%CO_2, standard error in the sensitivity estimate $s_{\hat{\beta}_1}$ in hPa, standard deviation of the noise S_ε in hPa, and lag-1 autocorrelation of the noise $\hat{\rho}$ in dimensionless units

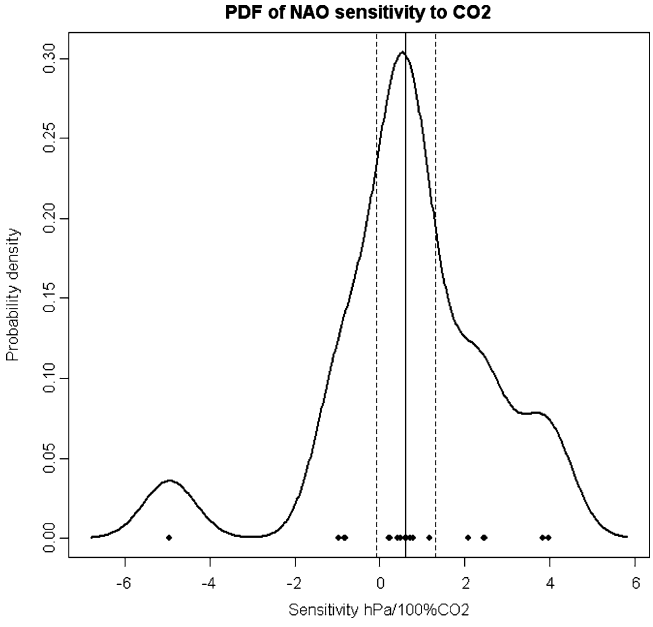

Fig. 5 Kernel estimate of the probability density function of model sensitivity of NAO to atmospheric carbon dioxide concentrations. The *filled circles* show the individual model estimates and the vertical lines show the multi-model median and 95% confidence interval (see text for details). Half the models (9 out of 18) are within the 95% confidence interval

rejected at the 5% level of significance. This does not imply that there is no effect – but it does state that the result could have been obtained as a result of chance sampling of sensitivities from this finite set of models. Assuming that the statistics obtained from the models here capture the true sensitivity, it is not unlikely to have models with negative sensitivities included in the sample. Thus, the comparatively high number of models in the present study gives more reliable statistics than previous studies, but still a zero sensitivity cannot be excluded.

Similar conclusions are obtained if the three models without NAO pressure dipole are removed (standard error in median of 0.0043 per $\%CO_2$) . Rejection of the models with high outlier sensitivities does not substantially reduce the confidence interval, for example, omission of the ECHAM4 model reduces the standard error in the model median from 0.0043 hPa per $\%CO_2$ for the 15 models able to simulate the NAO dipole to 0.0035 hPa per $\%CO_2$. This is very close to the interval estimate of 0.0036 hPa per $\%CO_2$ obtained for all 18 models. This is because the IQR is a measure of scale that is *resistant* to outliers so we do not need to exclude outlier models. If we had use standard deviation as a measure of scale then it might have been desirable to trim off the outliers first.

If even 18 models cannot be used to reject the no effect hypothesis, then extreme care should be exercised when judging even smaller subsets of models especially when they involve a predominance of models with extreme sensitivities such as ECHAM4 and HadCM3 (e.g. the 8 models in Gillett et al., 2003; the 7 models in Osborn 2004; and the 12 models in Kuzmina et al. 2005). Although the null hypothesis of no trend cannot be rejected here, this does not necessarily mean that it is true—there could be a real non-zero trend yet it fails to stand out from the background variation in sensitivities between models.

The weak sensitivity of the NAO index to changes in CO_2 atmospheric concentration is reflected also by the weak change in winter mean MSLP from 'control' to 'perturbed' experiments averaged over the last 20 years of integration (not shown). The maps of this quantity show a weak, statistically significant increase of the Azores high only for 6 models. All other changes are not statistically significant.

4 The Impact of the NAO response on European climate

This section presents the model predicted changes in winter mean temperature and precipitation and then uses a linear regression model to assess how much of these responses can be accounted for by the changes seen in NAO. For each response variable, the analysis consists of a description of the change occurred in each model winter climate when shifting from 'control' to 'perturbed' conditions. This includes both a description of the main characteristics of the total climate variation over the Euro-Atlantic region and of the contribution to it by NAO related impacts. After a general description of the changes observed over the whole Euro-Atlantic region, attention is focussed on the impacts of climate change on two regions: the Mediterranean and the Northern European region. In particular, the Mediterranean region (MED) extends from 10°W to 40°E and from 30°N to 48°N, while the Northern European region (NEU) extends from 10°W to 40°E and from 48°N to 75°N. The definition of these regions is the same as in IPCC (2001) and Giorgi and Francisco (2000).

4.1 Estimating the contribution of NAO

Following Hurrell (1995), we assume that winter mean temperature or precipitation responds linearly to changes in NAO:

$$Y = \alpha_0 + \alpha_1 X + \varepsilon_Y \tag{2}$$

where Y is the response variable (winter mean temperature or precipitation at a model grid point), X is the NAO index, and ε_Y is the part not accounted for by NAO. Ordinary Least Squares regression can be used to estimate the slope parameter and its standard error:

$$\hat{\alpha}_1 = \frac{s_{xy}}{s_x^2}$$
$$s_{\alpha_1} = \frac{1 - r^2}{\sqrt{n}} \frac{s_y}{s_x} \tag{3}$$

where s_x and s_x are the standard deviations of x and y, S_{xy} is the sample covariance of x and y, and r is the correlation of x and y. In this study, the sample size $n = 160$ since we chose to use winter means from both the control and perturbed simulations to estimate the slope parameter. To reduce sampling uncertainty, we prefer to use the whole record rather than just the control simulation (which gave similar results although a bit noisier) or short 20-year time slices (too short to estimate the covariance reliably).

The expected change in the response variable due to a change of Δx in NAO is then given by $\hat{\alpha}_1 \Delta x$ and this can be compared to the total change Δy observed in the response variable. In what follows, we consider the difference in means between the last 20 years of the perturbed simulation and the last 20 years of the control simulation. This is approximately the change one expects to occur by the end of the twenty-first century compared to late twentieth century present day conditions.

4.2 Surface temperature

Figure 6 shows the covariance of winter mean surface temperatures with the NAO index for each of the CONs. It is encouraging that all models are able to capture the well-known positive-negative temperature dipole pattern

between Greenland/Canada and Northern Europe. Figure 7 shows the difference between 'perturbed' and 'control' experiments for mean winter temperature averaged for each model over the last 20 years of integration. Grey shaded regions not statistically significant at the 5% level of significance have been identified using a 2-sample Student's t test on the 20-year means. All models show an increase in temperature over the Euro-Atlantic region, while only some models (BMRC2, CCCma1, CCSR, ECHAM3, GISS, INMCM, LMD/IPSL2, DOE_PCM and HadCM2) present a region of negative temperature change over the North Atlantic or Greenland. In general, maximum warming occurs over the Arctic region, with values that for some models can be as large as 10°C. Over Europe and the Mediterranean, the warming is generally rather uniform and around 1–2°C. However, some models show a strong increase in temperature over North Eastern Europe (CCCma1, CCSR, ECHAM3, ECHAM4, GFDL_R15a, LMD/IPSL2 and HADCM3).

Figure 8 shows the contribution $\hat{\alpha}_1 \Delta x$ of the temperature change that can be accounted for by changes in NAO over the last 20 years of the control and perturbed integrations. Grey shaded regions with slope parameters not statistically significant at the 5% level of significance have been identified using a Student t-test on the ratio $\hat{\alpha}_1 / s_{\alpha_1}$. For most models, the magnitude and spatial pattern of this change is substantially different from the total response shown in Fig. 7. Unlike the total response, the NAO contribution shows positive and negative changes in temperature of comparable magnitude in different regions. The magnitude of NAO related temperature changes over the European and Mediterranean region is much smaller (by typically a factor of 10) than the total change.

In order to quantify these findings, Tables 3 and 4 present statistics for area-average temperatures over the MED and NEU regions, respectively. In order to get the most reliable statistical estimates, all values in these tables were computed over the full 80 years of the control

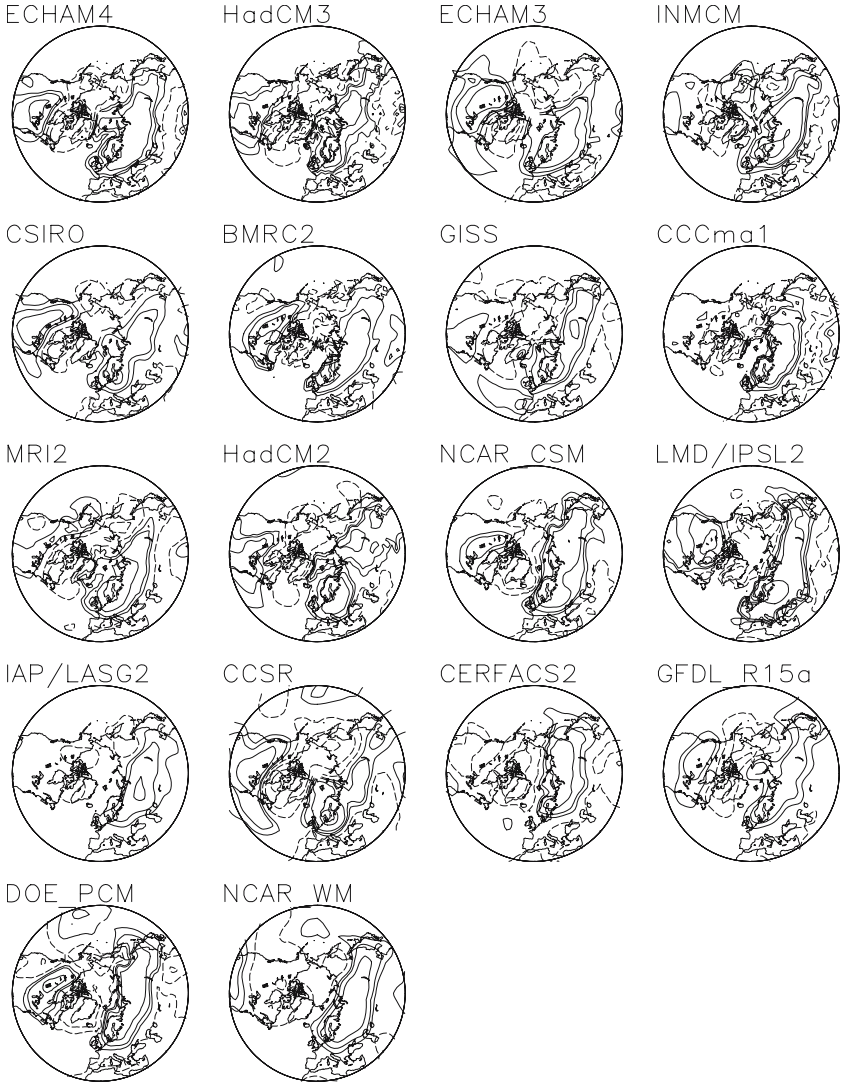

Fig. 6 Maps of covariance between surface air temperature and the standardised NAO indices for each of the control simulations. Contours marked at −5.0, −2.5, −1.0, −0.5, −0.25, 0.25, 0.5, 1.0, 2.5, and 5.0°C

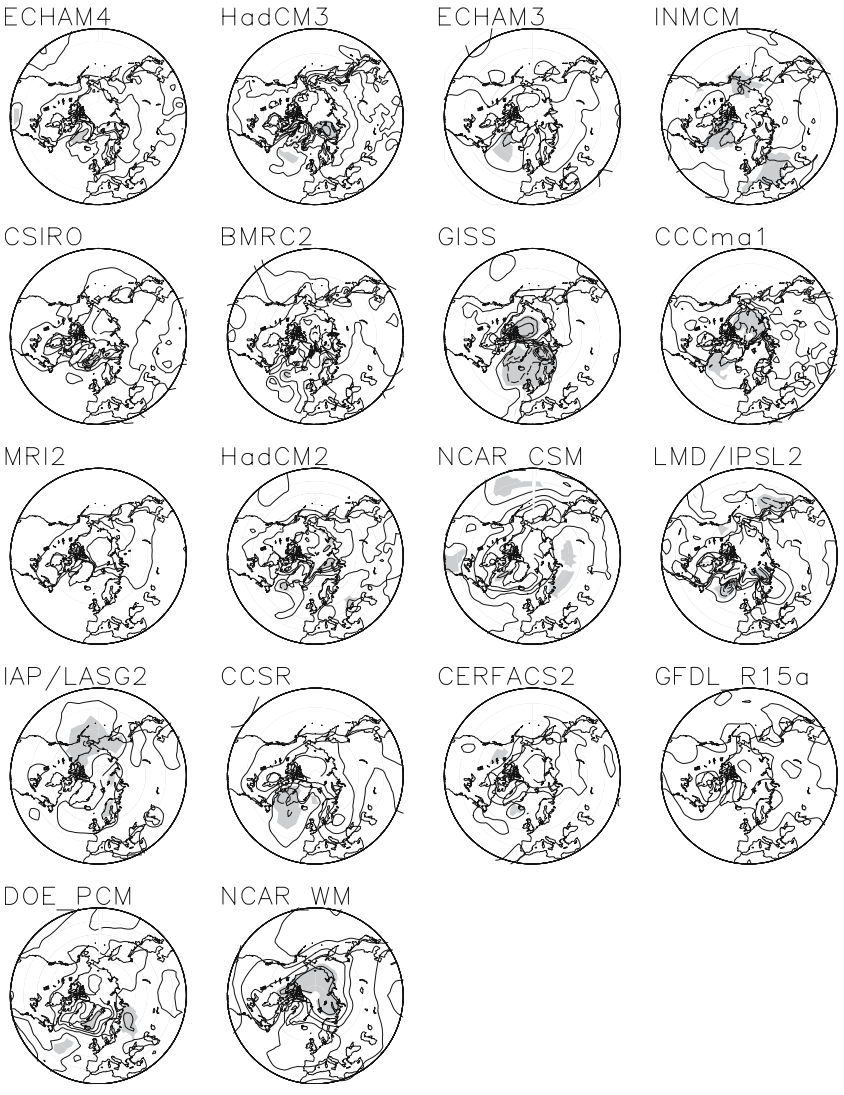

Fig. 7 Difference between the mean winter temperature in the last 20 years of the perturbed and control model simulations. Contours marked at −20, −15, −11, −7, −5, −3, −1, 1, 3, 5, 7, 11, 15, and 20°C with negative values *dashed* and positive values *solid*. Regions not statistically significant at the 5% level of significance are *grey shaded*

and perturbed simulation. The first column reports the values of the winter averaged surface temperature for observations (first row) and for the 'control' experiments, while the second contains the same winter averages, but for the 'perturbed' experiments. Compared with observations, most models show a cold bias over Northern Europe whereas only 10 out of 18 models show a cold bias over the Mediterranean region. Seven models are characterised by biases greater than 2°C over the MED region and 10 have a similarly intense bias over the NEU region. Comparing columns 1 and 2, it can be seen that all models produce an increase in mean winter temperature in 'perturbed' versus 'control' experiments. This increase is generally stronger in the NEU region as can be seen in Fig. 7. Columns 3 and 4 report the value of the trend, in degree per decades, computed for both 'control' and 'perturbed' experiments by applying the least square fit to the time series of winter averaged values. In the 'control' experiments, only a few models present substantial positive trends (greater than 0.1° per decade) in both MED and NEU, namely CERFACS2 and NCAR_WM, while others, like CCSR, ECHAM3, LMD/IPSL2, HadCM2 and HadCM3 present opposite trends over the two areas, or a moderate cooling over both areas, like BMRC2, GFDL_R15a and NCAR_CSM.

The covariance between NAO and surface air temperature (columns 5 and 6) is used to calculate the fraction of variance accounted for by NAO (columns 6 and 7). Most models, apart from CERFACS2 and IAP/LASG2 over NEU and LMD/IPSL2, NCAR_WM and HadCM2 over MED, overestimate both the covariance and the fraction of variance explained by NAO. Perturbed conditions generally produce a decrease in the fraction of variance explained by the NAO for all models apart from IAP/LASG2, NCAR_CSM, NCAR_WM and DOE_PCM. This suggests that the trends in surface air temperature in the perturbed simulations are not strongly related to changes in the NAO.

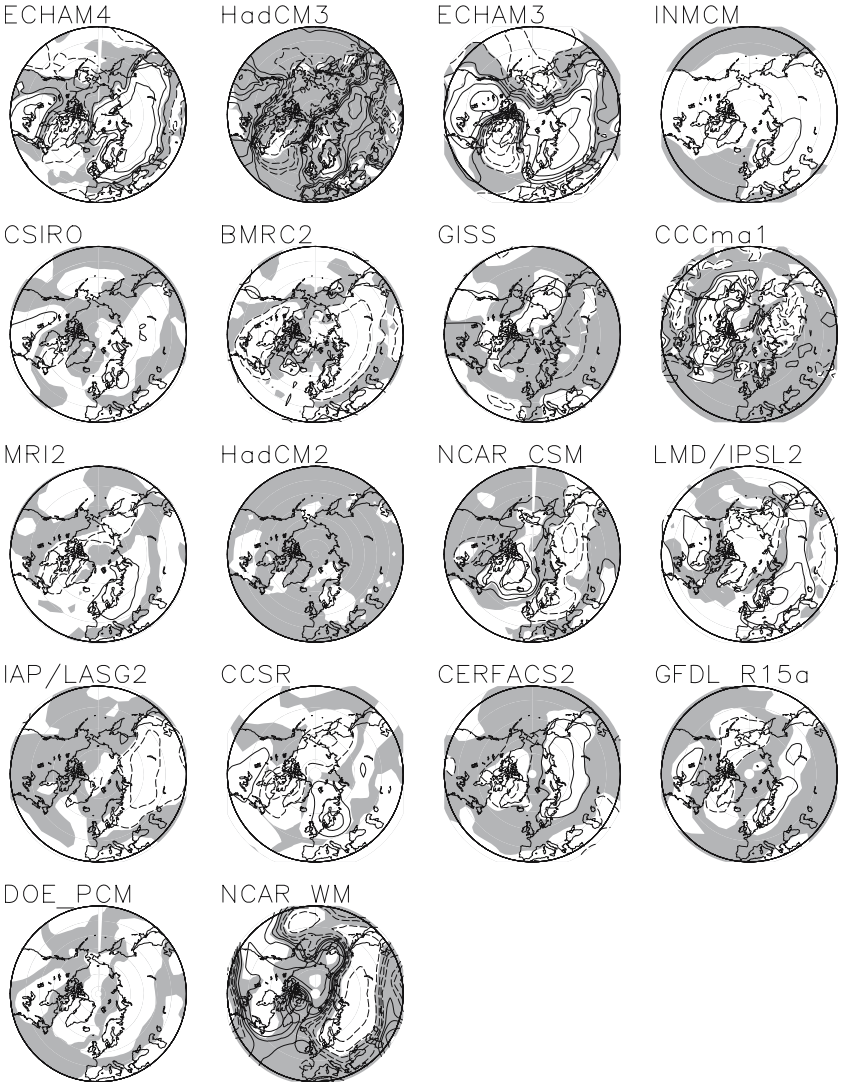

Fig. 8 NAO-explained difference between the mean winter temperature in the last 20 years of the perturbed and control model simulations. Contours marked at −5.0, −2.5, −1.0, −0.5, −0.25, −0.1, 0.1, 0.25, 0.5, 1.0, 2.5, and 5.0°C with negative values *dashed* and positive values *solid*. Regions not statistically significant at the 5% level of significance are *grey shaded*

4.3 Precipitation

Figure 9 shows the covariance of winter precipitation with the NAO index for each of the CONs. Encouragingly, all models are able to reproduce the north-south European dipole in NAO-related precipitation. Figure 10 shows the differences between mean precipitation in the last 20 years of the perturbed and control mean winter precipitation for each model. In most models, significant changes occur at high latitudes with an increase of wintertime precipitation along a band from the eastern North America across the North Atlantic up to Northern Europe. Unlike temperature, the precipitation response tends to have opposite sign over Europe with evidence of decreasing amounts of winter precipitation across southern Europe (e.g. the HadCM3 model).

Figure 11 shows the contribution $\hat{\alpha}_1 \Delta x$ of the precipitation change that can be accounted for by changes in NAO over the last 20 years of the control and perturbed integrations. Grey shaded regions with slope parameters not statistically significant at the 5% level of significance have been identified using a Student t-test on the ratio $\hat{\alpha}_1 / s_{\alpha_1}$. For each model the spatial pattern of this change exhibits similar characteristics to those of the total change, although the magnitude of the NAO contribution is much smaller than the total change.

Tables 5 and 6 summarise the results for precipitation averaged over the MED and NEU regions, respectively. The control simulations give a wide range of values for over the two regions. The range of values is broader for NEU than for MED, possibly due to the greater variability of precipitation over the NEU region. Over NEU, all models are wetter than observed, while 4 models out of 18 present a dry bias over MED. These biases in precipitation could be partly related to the mean NAO being too strong in most models. Comparison of columns 1 and 2 shows that all models predict the occurrence of an increase in precipitation over the NEU region, consistently with Fig. 7, while, in the MED region, three models predict an increase in mean winter precipitation (GFDL_R15a, NCARCSM and NCARWM), eight models a decrease (BMRC2, CCSR,

Table 3 Summary statistics for surface temperature averaged over the MED region: mean value, linear trend, covariance, fraction of total variance explained by NAO-related variability

Model	Mean (°C)		Trend (°C/decade)		Covariance (°C)		Explained var. (%)	
	CON	PER	CON	PER	CON	PER	CON	PER
Obs	9.13		0.005		−0.03		0.11	
BMRC2	10.22	10.95	−0.07	0.19	−0.18	−0.09	0.23	0.18
CCCma1	9.66	10.67	0.03	0.34	−0.13	0.14	0.20	0.15
CCSR	10.03	11.49	0.10	0.48	−0.48	−0.41	0.40	0.29
CERFACS2	11.54	12.25	0.09	0.33	−0.22	−0.18	0.27	0.17
CSIRO	8.77	10.22	0.01	0.39	−0.22	−0.22	0.30	0.22
ECHAM3	7.82	9.92	0.08	0.35	−0.13	0.06	0.25	0.20
ECHAM4	9.99	11.03	0.01	0.28	−0.08	0.14	0.28	0.17
GFDL_R15a	3.60	4.83	−0.06	0.16	−0.18	−0.21	0.18	0.17
GISS	11.50	12.21	−0.08	0.23	−0.19	−0.18	0.35	0.32
IAP/LASG2	6.73	7.33	−0.01	0.16	−0.07	0.11	0.15	0.15
INMCM	8.55	8.95	0.02	0.12	−0.16	−0.02	0.26	0.25
LMD/IPSL2	8.23	9.41	0.05	0.38	0.35	0.25	0.31	0.15
MRI2	10.92	11.83	0.04	0.30	−0.17	−0.17	0.36	0.26
NCAR_CSM	6.99	7.94	−0.05	0.21	−0.13	−0.39	0.33	0.39
NCAR_WM	11.76	13.46	0.13	0.66	0.007	−0.78	0.09	0.46
DOE_PCM	5.25	5.90	0.003	0.21	−0.23	−0.29	0.32	0.32
HadCM3	7.48	8.92	0.04	0.34	−0.38	−0.06	0.36	0.22
HadCM2	8.24	9.23	0.04	0.37	0.06	−0.23	0.25	0.24

All the statistics were estimated over the whole 80 years of the control and perturbed simulations

Table 4 Summary statistics for surface temperature averaged over the NEU region: mean value, linear trend, covariance, fraction of total variance explained by NAO-related variability

Model	Mean (°C)		Trend (°C/decade)		Covariance (°C)		Explained var. (%)	
	CON	PER	CON	PER	CON	PER	CON	PER
Obs	−1.51		0.002		0.23		0.15	
BMRC2	−1.71	−1.10	−0.06	0.17	0.61	0.84	0.36	0.42
CCCma1	0.95	2.39	−0.03	0.43	0.84	0.58	0.50	0.33
CCSR	−7.25	−4.78	−0.05	0.56	1.52	1.45	0.61	0.54
CERFACS2	1.05	2.07	0.12	0.32	0.22	0.23	0.17	0.18
CSIRO	−3.54	−1.55	0.08	0.45	0.57	0.64	0.37	0.39
ECHAM3	−4.55	−2.99	−0.06	0.51	1.04	1.20	0.56	0.58
ECHAM4	−2.10	−0.17	−0.07	0.49	1.17	1.12	0.55	0.53
GFDL_R15a	−4.29	−2.94	−0.04	0.58	0.37	0.44	0.28	0.23
GISS	−1.66	−1.64	−0.02	−0.03	0.68	0.47	0.45	0.32
IAP/LASG2	−2.64	−2.15	0.02	0.25	0.19	0.45	0.21	0.34
INMCM	−0.59	0.20	0.13	0.32	1.17	1.31	0.53	0.59
LMD/IPSL2	−6.34	−3.81	−0.10	0.49	1.26	0.85	0.43	0.30
MRI2	−0.54	0.63	0.05	0.34	1.14	0.97	0.62	0.53
NCAR_CSM	−6.99	−5.65	−0.06	0.39	0.78	0.91	0.44	0.40
NCAR_WM	1.03	2.94	0.45	0.96	0.63	−0.65	0.25	0.25
DOE_PCM	−5.87	−4.22	−0.18	0.35	0.88	0.97	0.41	0.39
HadCM3	−5.61	−3.31	−0.18	0.51	0.89	1.10	0.46	0.50
HadCM2	−1.80	−0.51	−0.09	0.29	1.09	0.83	0.58	0.43

All the statistics were estimated over the whole 80 years of the control and perturbed simulations

CSIRO, ECHAM3, ECHAM4, GISS, IAP/LASG2 and LMD/IPSL2) and seven a weak change (CCCma1, CERFACS2, INMCM, MRI2, DOE_PCM, HadCM2 and HadCM3). Over NEU, all models exhibit a larger trend in the PER of around 0.02–0.06 mm/day per decade, than in the CON. Over the MED area most models show a tendency to have more negative trends in the PERs than in the respective CONs. Exceptions are BMRC2, CSIRO, MRI2, NCAR_WM and DOE_PCM. Apart from DOE_PCM, these changes in the trends are consistent with changes in the mean values (columns 1 and 2): a decrease (increase) in the trend goes along with a reduced (increased) mean precipitation values in the PERs. Over the MED region, all models apart from BMRC2, CCCma1, LMD/IPSL2, MRI2, DOE_PCM and HadCM2 show a weak intensification of the covariance, its mean value becoming more negative in the perturbed simulations with respect to the control ones. At the same time, for this region, the fraction of total variance of precipitation explained by the NAO

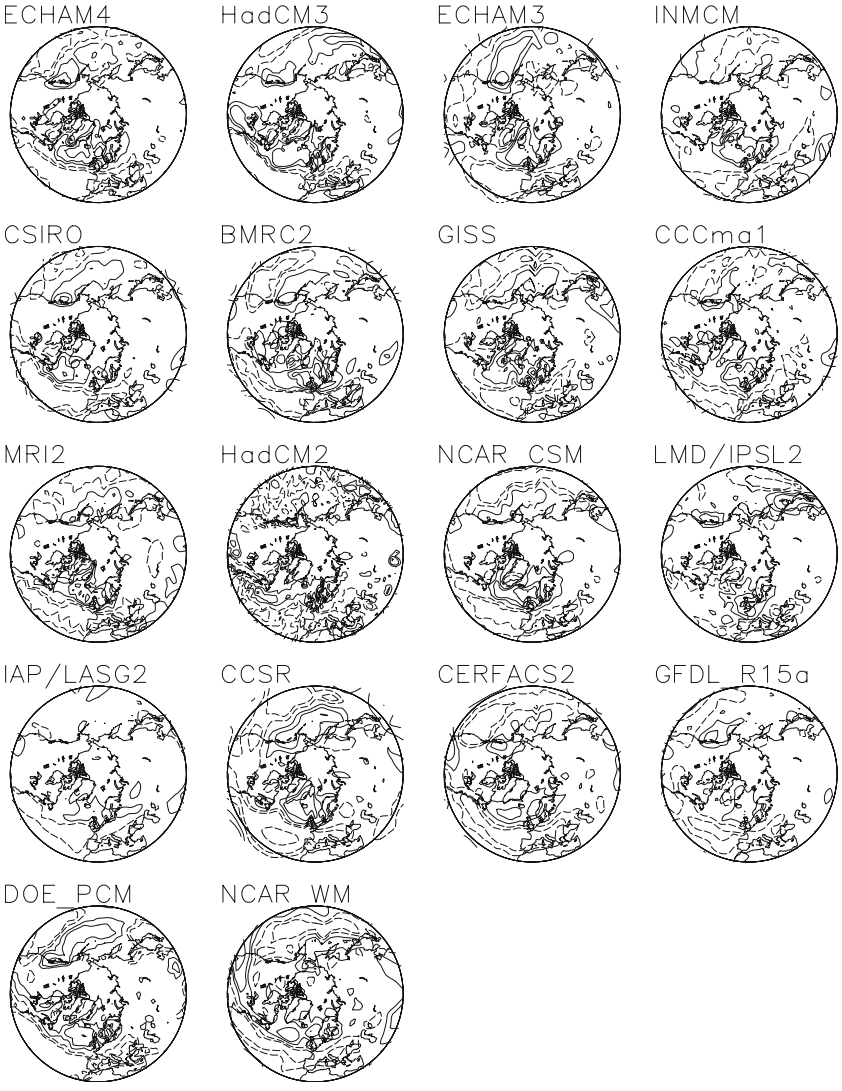

Fig. 9 Maps of covariance between precipitation grid point values and the standardised NAO indices for each of the control simulations. Contour lines marked at −5.0, −2.5, −1.0, −0.5, −0.25, −0.1, 0.1, 0.25, 0.5, 1.0, 2.5, and 5.0 mm/day

seems comparable for the two experiments for all models apart CCCma1, LMD/IPSL2 and NCAR_WM, suggesting that, if similar positive NAO anomalies produce stronger negative precipitation anomalies under perturbed conditions, also other processes produce comparable changes in precipitation variability over this region. The models presenting a more positive trend in precipitation over NEU (CSIRO, GFDL_R15a and NCAR_WM) are among those for which the covariance becomes more negative, suggesting that the other processes than NAO occur in these models to produce an increase in averaged precipitation during winter.

5 Conclusions

The main conclusions of this study are that:

- The majority of the coupled models (15 out of 18) are able to capture the gross spatial and temporal features of the winter mean NAO. Three out of 18 models are unable to capture the north–south dipole in SLP covariance;
- The models tend to overestimate the winter mean NAO—the Atlantic zonal winds are too strong and this is perhaps related to an overly strong polar vortex in the lower stratosphere as discussed by Castanheira and Graf (2003);
- None of the models in either the control or perturbed simulations are able to reproduce a decadal trend in NAO as strong as that observed from the 1960s to the 1990s. This confirms the results of Osborn (2004) based on only seven models;
- Fourteen out of the 15 models with NAO dipoles simulate an increasing trend in the NAO index with increasing amounts of carbon dioxide. This confirms similar findings by Rauthe et al. (2004) and Rauthe and Paeth (2004) for scenario experiments including not only changes in CO_2 but also in sulphate aerosols, and by Osborn (2004) and Gillett et al. (2003) for much smaller model sets of CO_2 scenario experiments;
- The magnitude of the response of NAO to carbon dioxide is generally small and very model-dependent. The multi-model median estimate is 0.0061 ± 0.0036 hPa per $\%CO_2$ (or 0.0072 ± 0.0043 hPa per % CO_2 if one

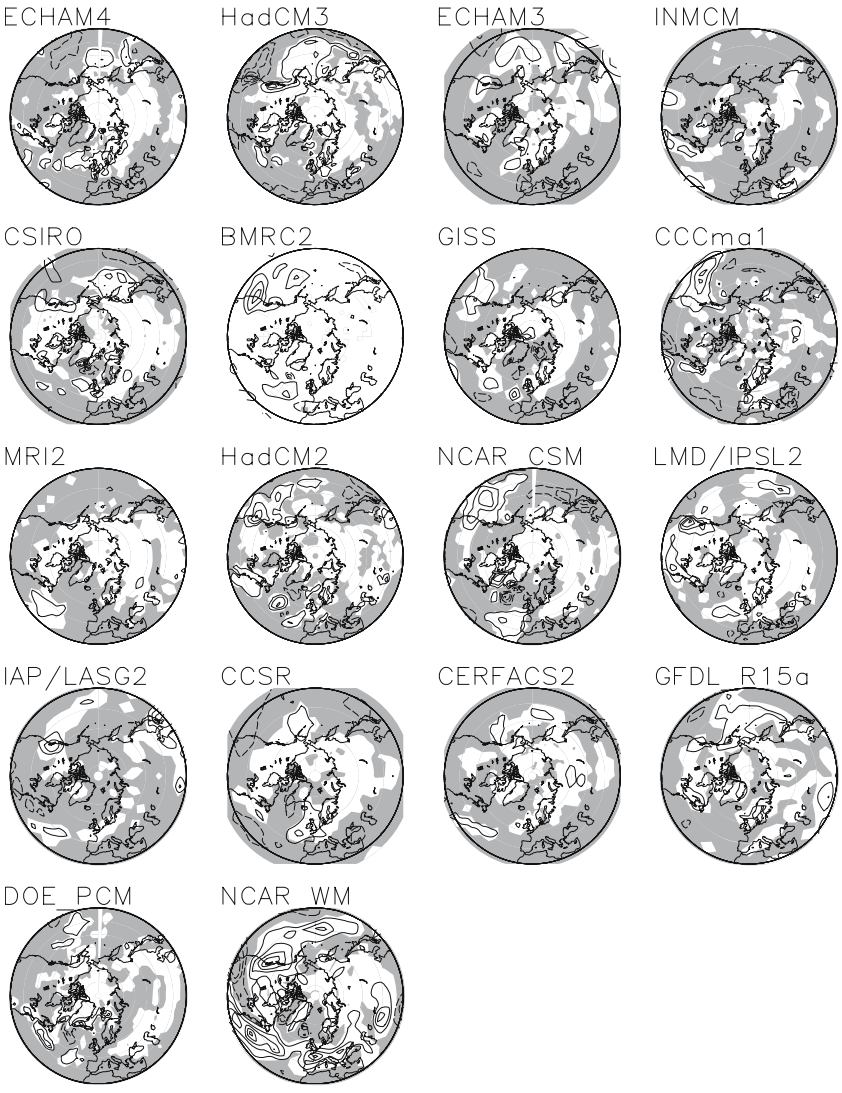

Fig. 10 Difference between the mean winter precipitation in the last 20 years of the perturbed and control model simulations. Contour interval of 0.5 mm/day with negative contours *dashed* and positive contours *solid* and zero contour line not shown. Regions not statistically significant at the 5% level of significance are *grey shaded*

excludes the three models without NAO pressure dipole) . There is a large amount of model uncertainty in the magnitude of the response. Several of the models are large outliers (e.g. ECHAM4, ECHAM3, HadCM3, and NCAR_WM) and so extreme care needs to be exercised when summarizing only a few models;

- Despite their different NAO responses, all models show a similar increasing NAO-like pattern in temperature and precipitation trends with increasing amounts of carbon dioxide: strong warming over most of Europe and increasing/decreasing precipitation in Northern/Southern Europe;
- Regression analysis shows that only a small fraction of the European temperature and precipitation changes can be attributed to the changes in NAO for all of the models. This confirms and generalises the conclusions of the high-latitude studies by Benestad (2001) and Overland and Wang (2005).

While it is encouraging that coupled models seem able to capture many of the main features of the NAO phenomenon, such as the interannual variability, it is disturbing that none of the 18 models were able to simulate sufficient decadal variability. Observed NAO is known to have more low-frequency variability than can be expected from a short-range process such as autoregressive noise (Stephenson et al. 2000). Furthermore, observed NAO exhibits long-range dependence both in recent times and in pre-industrial periods. In a recent coupled modelling study using HadCM3, Mosedale et al. (2005) demonstrated that model-simulated sea surface temperatures in a small region south of Cape Hatteras had a causal effect on model-simulated daily NAO, which then resulted in NAO trends on longer time scales. It is possible that the low-resolution coupled models are not fully resolving this key coupling process and thereby underestimate natural low-frequency trends in NAO. Alternatively, the observed trends in NAO may be the result of missing or poorly represented forcing factors such as changes in sea-ice or the stratosphere. This is supported by Scaife et al. (2005) who demonstrated a plausible stratospheric forcing of the observed NAO variations. Thus we must still however consider the possibility that the large decadal fluctuations in NAO

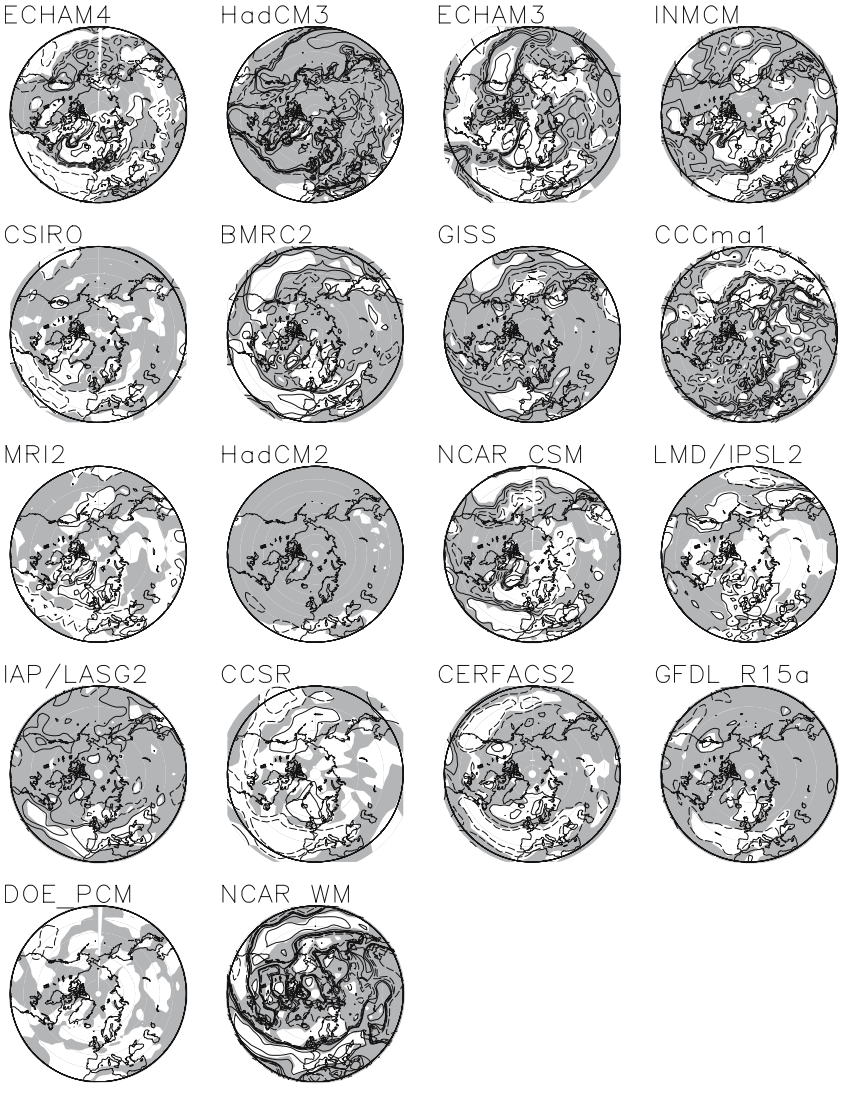

Fig. 11 NAO-explained difference between the mean winter precipitation in the last 20 years of the perturbed and control model simulations. Contours marked at −5.0, −2.5, −1.0, −0.5, −0.2, −0.05, −0.02, 0.02, 0.05, 0.2, 0.5, 1.0, 2.5, and 5.0 mm/day with negative values *dashed* and positive values *solid*. Regions not statistically significant at the 5% level of significance are *grey shaded*

might be an extreme manifestation of stochastic natural variability and/or a response to changes in forcing via mechanisms missing in the models.

The model simulations suggest that NAO shows a weak positive response to increasing amounts of carbon dioxide. Although an increase of 0.61 hPa (all 18 models) or 0.72 hPa (the 15 models with NAO SLP dipole) in NAO for a doubling in CO_2 represents only a relatively small shift of 0.18 or 0.21 standard deviations, respectively, in the probability distribution of winter mean NAO, this can cause large relative increases in the probabilities of extreme values of NAO associated with damaging impacts. However, the amplitude (and sign!) of the response varies widely across the models with several models being clear outliers. For example, the ECHAM4, ECHAM3, HadCM3, and NCAR_WM models have much larger and more atypical responses than many of the other models yet these models contributed to several of the previous smaller multi-model NAO studies. However, one might argue that NCAR_WM should not be included since it was unable to simulate the NAO SLP Atlantic dipole. With such large amounts of model uncertainty, one has to be exceedingly careful about making inferences concerning future climate change. Even with 18 coupled models, it is not possible to reject the null hypothesis of no NAO response to carbon dioxide at the 5% level of statistical significance. With only a small finite number of not truly independent coupled models, this raises a problem that needs to be surmounted in order for climate change predictions of NAO to be believable. Recent developments and equilibrium and transient ensemble climate change prediction using the ''perturbed physics'' approach may prove successful in this regard (Murphy et al. 2004; Stainforth et al. 2005; Collins et al. 2006). Nevertheless, detailed and novel modelling studies are required to understand and quantify the sources of the uncertainties.

It is reassuring to note that despite their differences in NAO response, the coupled models give more similar responses in temperature and precipitation over Europe. This suggests that NAO is not the key determining factor for such changes. However, it should be noted that not all the changes in the flow pattern relevant for

Table 5 Summary statistics for precipitation averaged over the MED region: mean value, linear trend, covariance, fraction of total variance explained by NAO-related variability

Model	Mean mm/day		Trend mm/day/decade		Covariance mm/day		Explained var. (%)	
	CON	PER	CON	PER	CON	PER	CON	PER
Obs	1.68		−0.025		−0.22		0.20	
BMRC2	1.80	1.66	−0.04	−0.03	−0.15	−0.11	0.25	0.22
CCCma1	1.75	1.72	0.002	0.001	−0.11	−0.08	0.29	0.16
CCSR	1.51	1.44	0.02	−0.01	−0.12	−0.13	0.23	0.22
CERFACS2	1.84	1.85	0.01	−0.01	−0.20	−0.26	0.31	0.36
CSIRO	1.77	1.72	−0.02	−0.002	−0.11	−0.14	0.31	0.31
ECHAM3	1.38	1.29	0.004	−0.03	−0.19	−0.21	0.40	0.40
ECHAM4	2.35	2.29	0.02	−0.02	−0.20	−0.21	0.31	0.31
GFDL_R15a	2.15	2.23	0.001	−0.04	−0.07	−0.10	0.21	0.23
GISS	1.90	1.82	−0.03	−0.05	−0.14	−0.13	0.12	0.10
IAP/LASG2	1.64	1.56	−0.003	−0.04	−0.06	−0.10	0.17	0.22
INMCM	2.08	2.06	-0.01	−0.01	−0.11	−0.15	0.26	0.30
LMD/IPSL2	1.90	1.80	0.01	−0.02	−0.06	−0.06	0.31	0.23
MRI2	1.88	1.86	0.01	0.01	−0.12	−0.10	0.42	0.40
NCAR_CSM	1.92	1.98	−0.001	−0.01	−0.14	−0.17	0.32	0.35
NCAR_WM	2.78	2.93	0.003	0.07	−0.12	−0.19	0.20	0.31
DOE_PCM	1.51	1.49	0.002	0.01	−0.09	−0.09	0.11	0.09
HadCM3	1.90	1.88	0.004	−0.02	−0.10	−0.15	0.08	0.09
HadCM2	1.94	1.91	0.01	−0.01	−0.18	−0.16	0.11	0.08

All the statistics were estimated over the whole 80 years of the control and perturbed simulations

Table 6 Summary statistics for precipitation averaged over the NEU region: mean value, linear trend, covariance, fraction of total variance explained by NAO-related variability

Model	Mean mm/day		Trend mm/day/decade		Covariance (mm/day)		Explained var. (%)	
	CON	PER	CON	PER	CON	PER	CON	PER
Obs	1.47		0.01		0.06		0.20	
BMRC2	3.05	3.25	0.02	0.04	0.18	0.20	0.26	0.30
CCCma1	2.57	2.70	0.01	0.05	0.11	0.11	0.27	0.21
CCSR	2.28	2.46	−0.02	0.04	0.11	0.09	0.32	0.28
CERFACS2	3.49	3.63	0.01	0.06	0.06	0.17	0.32	0.39
CSIRO	2.23	2.40	0.01	0.03	0.01	0.08	0.20	0.30
ECHAM3	2.6	2.73	−0.003	0.05	0.14	0.16	0.32	0.32
ECHAM4	2.59	2.79	−0.004	0.05	0.13	0.17	0.31	0.37
GFDL_R15a	2.39	2.44	−0.01	0.03	0.06	0.07	0.20	0.16
GISS	2.51	2.58	0.003	0.06	0.01	0.05	0.13	0.09
IAP/LASG2	2.14	2.23	−0.01	0.02	0.07	0.07	0.18	0.17
INMCM	2.28	2.34	0.01	0.02	0.05	0.13	0.33	0.36
LMD/IPSL2	2.27	2.39	0.01	0.05	0.13	0.12	0.40	0.34
MRI2	2.58	2.66	−0.01	0.02	0.12	0.13	0.34	0.34
NCAR_CSM	2.56	2.62	−0.01	0.02	0.22	0.19	0.45	0.41
NCAR_WM	3.86	3.99	−0.02	0.04	0.10	0.07	0.22	0.17
DOE_PCM	2.56	2.62	−0.004	0.02	0.12	0.10	0.16	0.17
HadCM3	2.26	2.43	0.003	0.04	0.05	0.13	0.06	0.07
HadCM2	2.34	2.42	−0.02	0.03	0.06	0.04	0.08	0.08

All the statistics were estimated over the whole 80 years of the control and perturbed simulations

local rainfall or temperature over the North Atlantic and Europe are completely captured by the crude NAO index used here. This study has tested the NAO response by using a regression model to quantify how much NAO accounts for such changes though if the models lack key processes, their inclusion could lead to this conclusion being modified. Different processes can lead to similar temperature and precipitation patterns over Europe – there is degeneracy in the response. One possible explanation for the degeneracy is that both fluid dynamic (i.e. NAO) and thermodynamic processes can modulate the storms that transport heat and moisture to Europe in winter. The spatial pattern of the temperature and precipitation response is determined by the spatial orientation of the storm track. If everything else remains constant (e.g. NAO), then warmer conditions will lead to a storm track that transports more heat and moisture over Europe.

Acknowledgements MMJ was funded by the Deutsche Forschungsgemeinschaft, Bonn, Germany, through the Sonderforschungsbereich 512: Tiefdruckgebiete und Klimasystem des Nordatlantiks and by the Italian national project SINAPSI. This work was also partially funded under the European projects STARDEX (*Sta*tistical and *R*egional dynamical *D*ownscaling of *Ex*tremes) under contract number EVK2-CT-2001-00115, ENSEMBLES (GOCE-CT-2003-505539) and DYNAMITE (GOCE-003903). MC was supported by the UK Department of the Environment, Food and Rural Affairs under Contract PECD/7/12/37.

References

Alexander LV, Jones PD (2001) Updated precipitation series for the UK and discussion of recent extremes. Atmos Sci Lett 1:142–150

Alexander MA, Bhatt US, Walsh J, Timlin M, Miller J (2004) The atmospheric response to realistic Arctic Sea Ice anomalies in an AGCM during winter. J Clim 17:890–905

Ambaum MH, Hoskins BJ, Stephenson DB (2001) Arctic Oscillation or North Atlantic Oscillation? J Clim 14:3495–3507

Ambaum MHP, Hoskins BJ, Stephenson DB (2002) Corrigendum: Arctic Oscillation or North Atlantic Oscillation? J Clim 15:553

Barnston AG, Livezey RE (1987) Classification, seasonality and persistence of low-frequency atmospheric circulation patterns. Mon Weather Rev 115:1083–1126

Benestad RE (2001) The cause of warming over Norway in the ECHAM4/OPYC3 GHG integration, Int J Climatol 21(3):371–387

Bojariu R (1992) Air temperature over Europe associated to certain oscillating type atmospheric phenomena. Meteorol Hydrol 22:29–32

Branstator G (2002) Circumglobal teleconnections, the jet stream waveguide, and the North Atlantic Oscillation. J Clim 15:1893–1910

Castanheira JM, Graf H-F (2003) North Pacific–North Atlantic relationships under stratospheric control? J Geophys Res 108:4036. DOI 10.1029/2002JD002754

Chambers JM, Cleveland WS, Kleiner B, Tukey PA (1983) Graphical methods for data analysis. Wadsworth & Brooks/Cole, USA

Cleveland WS (1979) Robust locally weighted regression and smoothing scatterplots. J Am Stat Assoc 74:829–836

Cohen J, Frei A, Rosen RD (2005) The role of boundary conditions in AMIP-2 simulations of the NAO, J Clim 18(7):973–981

Collins M, Booth BBB, Harris GR, Murphy JM, Sexton DMH, Webb MJ (2006) Towards quantifying uncertainty in transient climate change. Clim Dyn (in press)

Conway D, Wilby RL, Jones PD (1996) Precipitation and air flow indices over the British Isles. Clim Res 7:169–183

Dai A, Fung IY, Del Genio AD (1997) Surface observed global land precipitation variations during 1900–88. J Clim 10:2943–2962

Deser C, Blackmon ML (1993) Surface climate variations over the North Atlantic Ocean during winter: 1900–1989. J Clim 10:393–408

Doblas-Reyes FJ, Pavan V, Stephenson D (2003) The skill of multi-model seasonal forecasts of the wintertime North Atlantic Oscillation. Clim Dyn 21:501–514

Draper NR, Smith H (1998) Applied regression analysis, 3rd edn. Wiley, pp 736

Feldstein SB (2002) The recent trend and variance increase of the annular mode. J Clim 15:88–94

Furevik T, Bentsen M, Drange H, Kindem IKT, Kvamstø G, Sorteberg A (2003) Description and validation of the Bergen Climate Model: ARPEGE coupled with MICOM. Clim Dyn 21:27–51. DOI 10.1007/s00382-003-0317-5

Fyfe JC, Boer GJ, Flato GM (1999) The Artic and Antarctic Oscillations and their projected changes under global warming. Geophys Res Lett 26:1601–1604

Gillett NP, Zwiers FW, Weaver AJ, Hegerl GC, Allen MR, Stott PA (2002) Detecting anthropogenic influence with a multi-model ensemble. Geophys Res Lett 29(20):1970. DOI 10.1029/2002GL015836

Gillett NP, Zwiers FW, Weaver AJ, Stott PA (2003) Detection of human influence on sea-level pressure. Nature 422:292–294

Giorgi F, Francisco R (2000) Uncertainties in regional climate change prediction: a regional analysis of ensemble simulations with the HADCM2 coupled AOGCM. Clim Dyn 16:169–182

Glowienka-Hense R (1990) The North Atlantic Oscillation in the Atlantic–European SLP. Tellus 42A:497–507

Harrison MSJ, Palmer TN, Richardson DS, Buizza R, Petroliagis T (1996) Joint ensembles from the UKMO and ECMWF models. In: European Centre for Medium-Range Weather Forecasts (ed) On proceedings of ECMWF seminar on predictability, 4–8 September 1995

Holland MM (2003) The North Atlantic Oscillation—Arctic oscillation in the CCSM2 and its influence on Arctic climate variability. J Clim 16:2767–2781

Hu ZZ, Wu ZH (2004) The intensification and shift of the annual North Atlantic Oscillation in a global warming scenario simulation, Tellus Series A 56(2):112–124

Hurrell JW (1995) Decadal trends in the North Atlantic Oscillation: regional temperatures and precipitation. Science 269:676–679

Hurrell JW, van Loon H (1997) Decadal variations in climate associated with the North Atlantic Oscillation. Clim Change 36:301–326

Hurrell JW, Hoerling MP, Phillips AS, Xu T (2004) Twentieth century North Atlantic climate change. Part 1: assessing determinism. Clim Dyn 23(3–4):371–389

IPCC (2001) Climate Change 2001: Synthesis Report. In: Watson RT, Core Writing Team (eds) Cambridge University Press, Cambridge, 398 pp

Jones PD, Raper SCB, Bradley RS, Diaz HF, Kelly PM, Wigley TML (1986) Northern hemisphere surface air temperature variations, 1851–1984. J Clim Appl Meteorol 25:161–179

Krishnamurti TN, Kishtawal CM, Timoty EL, Bachiochi DR, Zhang Z, Williford CE, Gadgil S, Surendran S (1999) Improved weather and seasonal climate forecasts from multimodel superensemble. Science 285:1548–1550

Kuzmina SI, Bengtsson L, Johannenssen OM, Drange H, Bobylev LP, and Miles MW (2005) The North Atlantic Oscillation and greenhouse-gas forcing. G.R.L. 32:L04703. DOI 10.1029/2004GL021064

Kvamsto NG, Skeie P, Stephenson DB (2004) Impact of Labrador sea-ice on the North Atlantic Oscillation, Int J Clim 24:603–612

Lamb PJ, Peppler RA (1987) North Atlantic Oscillation: concept and an application. Bull Am Meteor Soc 68:1218–1225

Liu XY, Zhang XH, Yu YQ,Yu RC (2004) Mean climate characteristics in high northern latitudes in an ocean-sea ice-atmosphere coupled model. Adv Atmos Sci 21:236–244

Marshall J, Kushnir Y, Battisti D, Chang P, Czaja A, Dickson R, Hurrell J, McCartney M, Saravanan R, Visbeck M (2001) North Atlantic climate variability: phenomena, impacts and mechanisms. Int J Climatol 21:1863–1898

Meehl GA, Boer GJ, Covey C, Latif M, Stouffer RJ (2000) The coupled model intercomparison project (CMIP). Bull Am Met Soc 81:313–318

Min S-K, Legutke S, Hense A, Kwon W-T (2005) Internal variability in a 1000-year control simulation with the coupled climate model ECHO-G. II: El Niño Southern Oscillation and North Atlantic Oscillation. Tellus 57A:622–640

Mosedale TJ, Stephenson DB, Collins M, and Mills TC (2005) Granger causality of coupled climate processes: ocean feedback on the North Atlantic Oscillation. J Clim (in press)

Mosedale TJ, Stephenson DB, Collins M, and Mills TC (2006) Granger causality of coupled climate processes: ocean feedback on the North Atlantic Oscillation. J Clim 19(7):1182–1194

Murphy JM, Sexton DMH, Barnett DN, Jones GS, Webb MJ, Collins M, Stainforth DA (2004) Quantification of modelling uncertainties in a large ensemble of climate change simulations. Nature 430:768–772

Osborn TJ (2002) The winter North Atlantic Oscillation: roles of internal variability and greenhouse gas forcing. Exchanges, pp 25

Osborn TJ (2004) Simulating the winter North Atlantic Oscillation: the roles of internal variability and greenhouse gas forcing. Clim Dyn 22:605–623

Osborn TJ, Briffa KR, Tett SFB, Jones PD, Trigo RM (1999) Evaluation of the North Atlantic Oscillation as simulated by a coupled climate model. Clim Dyn, 15:685–702

Overland JE, Wang M (2005) The Arctic climate paradox: The recent decrease of the Arctic Oscillation, Geophys Res Lett 32 (6): art. no. L06701

Paeth H, Hense A, Glowienka-Hense R Voss R (1999) The North Atlantic Oscillation as an indicator for greenhouse-gas induced regional climate change. Clim Dyn 15:953–960

Palmer TN, Branković Č, Richardson DS (2000) A probability and decision-model analysis of PROVOST seasonal multi-model ensemble integrations. Q J Meteorol Soc, 126:2013–2033

Pavan V, Doblas-Reyes F (2000) Multi-model seasonal hindcasts over the Euro-Atlantic: skill scores and dynamic features. Clim Dyn 16:611–625

Pavan V, Marchesi S, Morgillo A, Cacciamani C, Doblas-Reyes FJ (2005) Downscaling of DEMETER winter seasonal hindcasts over Northern Italy. Tellus 57A:424–434

Pittalwala II, Hameed S (1991) Simulation of the North-Atlantic Oscillation in a general-circulation model. Tellus 18(5):841–844

Plaut G, Simonnet E (2001) Large-scale circulation classification, weather regimes, and local climate over France, the Alps and Western Europe. Climate Res 17:303–324

Rauthe M, Paeth H (2004) Relative importance of Northern Hemisphere Circulation models in predicting regional climate change. J Clim 17:4180–4189

Rauthe M, Hense MA, Paeth H (2004) A model intercomparison study of climate change signals in the extratropical circulation. Int J Climatol 24:643–662

Rodò X, Baert E, Comin FA (1997) Variations in seasonal rainfall in Southern Europe during the present century: relationship with the North Atlantic Oscillation and the El Niño-Southern Oscillation. Clim Dyn 13:275–284

Scaife AA, Knight JR, Vallis GK, and Folland CK (2005) A stratospheric influence on the winter NAO and North Atlantic surface climate, Geophys Res Lett 32:L18715. DOI 10.1029/2005GL023226

Slonosky VC, Yiou P (2001) the North Atlantic Oscillation and its relationship with near surface temperature. Geophys Res Lett 28:807–810

Stainforth DA, Aina T, Christensen C, Collins M, Faull N, Frame DJ, Kettleborough JA, Knight S, Martin A, Murphy JM, Piani C, Sexton D, Smith LA, Spicer RA, Thorpe AJ, Allen MR (2005) Uncertainty in predictions of the climate response to rising levels of greenhouse gases. Nature 433:403–406

Stenchikov G, Robock A, Ramaswamy V, Schwarzkopf MD, Hamilton K, Ramachandran S (2002) Arctic oscillation response to the 1991 Mount Pinatubo eruption: effects of volcanic aerosols and ozone depletion. J Geophys Res 107(D24):4803. DOI 10.1029/2002JD002090

Stephenson DB, Pavan V (2003) The North Atlantic Oscillation in coupled climate models: a CMIP1 evaluation. Clim Dyn 20:381–399

Stephenson DB, Pavan V, Bojariu R (2000) Is the North Atlantic Oscillation a random walk? Int J Climatol 20:1–18

Stephenson DB, Wanner H, Broennimann S, Luterbacher J (2002) The History of Scientific Research on the North Atlantic Oscillation. In: Hurrell JW, Kushnir Y, Ottersen G, Visbeck M (eds) The North Atlantic Oscillation: climatic significance and environmental impact. Geophysical Monograph 134, American Geophysical Union, Washington, pp 37–50

Terray L, Demory M.-E, Deque M, de Coetlogon G, Maisonnave E (2004) Simulation of late twenty-first century changes in wintertime atmospheric circulation over Europe due to anthropogenic causes. J Clim 17(24):4630–4635

Thompson DWJ, Wallace JM (2001) Regional climate impacts of the Northern Hemisphere annular mode. Science 293:85–89

Trenberth KE, Paolino DA Jr (1980) The Northern Hemisphere sea-level pressure data set: Trends, errors and discontinuities. Mon Wea Rev 108:855–872

Trigo IF, Davies TD, Bigg GR (2000) Decline in Mediterranean rainfall caused by weakening of Mediterranean cyclones. Geophys Res Lett 27(28):2913–2916

Ulbrich U, Christoph M (1999) A shift of the NAO and increasing storm track activity over Europe due to anthropogenic greenhouse gas forcing. J Clim 15(7):551–559

Venables WN, Ripley BD (2002) Modern applied statistics with S. Springer, Berlin Heidelberg New York

Wallace JM, Zhang Y, Bajuk L (1996) Interpretation of interdecadal trends in Northern Hemisphere surface air temperature. J Clim 9:249–259

Wanner H, Bronnimann S, Casty C, Gyalistras D, Luterbacher J, Schmutz C, Stephenson DB, Xoplaki E (2001) North Atlantic Oscillation—concepts and studies. Surv Geophys 22:321–382

The WASA Group (1998) Changing waves and storms in the Northeast Atlantic? Bull Am Met Soc 79:741–760

Wibig J (1999) Precipitation in Europe in relation to circulation patterns at the 500 hPa level. Int J Climatol 19:253–269

Xie P, Arkin PA (1996) Analyses of global monthly precipitation using gauge observations, satellite estimates and numerical model predictions. J Clim 9:840–858

Zhou T, Zhang X-H, Yu Y-Q, Yu R, Wang S (2000) The North Atlantic Oscillation simulated by versions 2 and 4 of IAP/LASG GOALS Model. Adv Atmos Sci 17(4):601–616

Zorita E, Gonzàlez-Rouco F (2000) Disagreement between predictions of the future behaviour of the Arctic Oscillation as simulated in two different climate models: implications for global warming. Geophys Res Lett 27:1755–1758